Microbial Pb(II) removal: modelling the role of passive mechanisms

Brandon van Veenhuyzen

November 3, 2020

Contents

Chapter 1

Theory

1.1 Background

1.1.1 Lead and the environment

Five million tons of lead (Pb) ore are mined annually to be refined for use in a variety of industrial applications (ILA, 2019). The most common application of Pb is in the manufacturing of Pb acid batteries for energy storage. These batteries are mostly utilized in automotive applications as well as emergency power supplies for various critical services such as hospitals, communication networks, public buildings, and emergency services. Additionally, Pb batteries arguably form the backbone of renewable energy industries such as solar photo-voltaic implementations, wind turbines, and electric or hybrid vehicles. The extremely high density of Pb provides unrivalled radiation protection which is essential for medical, dental, research, and nuclear installations. Further, Pb is used as a stabilizer to increase the durability of PVC products and has been applied to thousands of kilometres of underwater power and communication cabling (ILA, 2019).

Two problems, however, arise from lead industries. Firstly, the present rate of lead extraction considered with the most recent estimate of current lead ore reserves (88 Mt) means that raw lead could potentially be depleted by 2035 (Statista, 2019). Secondly, these industries introduce lead pollutants into the environment. This includes drainage and tailings from mining, waste water streams and spillage from processing, and landfill leachate from the disposal of Pb-containing products (UNEP, 2010; Van Hille et al., 2003). The most concerning form of lead pollution is in ionic or aqueous form: Pb(II). In this oxidation state it is soluble in water and more likely to form organic complexes or attach to colloidal particles, making it exceptionally mobile and available for interfer-

ence in biological processes (Naik and Dubey, 2013). A compilation of sampled effluent Pb(II) concentrations are given in Table 1.1.

Table 1.1: Concentration of aqueous lead in various industrial waste waters. Source: Verma et al. (2016).

Industry	Effluent concentration ($mg\,L^{-1}$ Pb^{2+})
Chemical manufacturing plant	326
Oil	125 - 250
Battery manufacturing	5 - 15
Electroplating	116
Industrial plant	19.1

Lead is highly toxic and has been found to accumulate through different trophic levels of ecosystems (Naik and Dubey, 2013). Lead could therefore be present in sub-lethal quantities in water but concentrate to lethal doses within the food chain (Van Hille et al., 2003). Lead serves no biological purpose, but rather harms organisms by disrupting the electron transport chain (Okoro et al., 2011), damaging membranes (Patra et al., 2011) and denaturing proteins (Gadd and Griffiths, 1977), impairing enzymes (Yang, Liu, et al., 2006), and substituting cationic nutrients (Okoro et al., 2011). Exposure to toxic heavy metals has also been found to stunt growth in organisms as cellular energy is redirected towards mechanisms of repair and resistance (Knops et al., 2001). In plants, lead exposure results in necrosis, the inhibition of growth, and a reduction in biomass (Shakoor et al., 2013). For animals, this harm is seen in the form of damage done to the central nervous system, kidneys, reproductive and immune system (UNEP, 2010).

Cases of lead poisoning have been reported in local communities close to lead-acid battery recycling plants, lead transportation routes, and lead ore mines (Shakoor et al., 2013). In humans, exposure to high concentrations of lead has been shown to cause neuronal encephalopathy and gastrointestinal colic, which includes symptoms such as constipation, abdominal pain, and intestinal paralysis (Mudipalli, 2007).

Lead, lead dioxide, and lead sulfate are classified as very or extremely hazardous wastes in South Africa. These compounds are considered to pose acceptable risks in the environment only at concentrations below $0.1\,mg\,L^{-1}$ and can only be disposed of at a monthly amount of less than $151\,g\,ha^{-1}$ in an immobilised or encapsulated form (Department of Water Affairs and Forestry, 1998).

Guidelines for the upper limit of lead in water for various uses are given in Table 1.2.

Table 1.2: Water quality targets for lead in various uses of water. Adapted from Department of Water Affairs and Forestry (1998).

Category of water use	Upper limit ($mg\,L^{-1}$ Pb^{2+})
Domestic	0.01
Irrigation	0.2
Livestock watering	0.1
Aquatic ecosystems	0.06

1.1.2 Current heavy metal removal technology

Various processes are available to remove Pb(II) from industrial effluent. A summary of the most widely employed techniques is presented in Table 1.3. Although the established use of these methods make them favourable, recurring disadvantages of these processes include high operating and maintenance costs as well as the need to further treat the concentrate of heavy metal produced.

Table 1.3: Conventional techniques employed for removing heavy metal from water. Compiled from Fu and Wang (2011), Van Hille et al. (2003), and Edzwald (2011).

Treatment strategy	Description	Advantages	Disadvantages
Chemical precipitation	Compounds are added to water to react heavy metals into a less soluble form.	Fast kinetics, simple operation.	Sludge generation and poor efficiency with effluents of low metal concentration.

Table 1.3: Conventional techniques employed for removing heavy metal from water. Compiled from Fu and Wang (2011), Van Hille et al. (2003), and Edzwald (2011).

Treatment strategy	Description	Advantages	Disadvantages
Ion exchange	Heavy metals are swapped for benign counter-ions from an exchange resin.	Rapid operation, high selectivity and treatment capacity.	Sensitive to sulfates and dissolved solids, large volumes of regenerant to be disposed of.
Pressure driven membrane filtration	Treatments such as reverse osmosis that force water through a membrane which rejects heavy metals.	High efficiency and selectivity.	High operating and maintenance costs. Heavy metal concentrate requires safe disposal.
Adsorption	Heavy metals in the aqueous phase bind to the surface of a solid.	Low capital cost, solids can be regenerated.	Low selectivity. Desorption process required to recover heavy metals.
Electrochemical treatment	An applied current causes the deposition of heavy metals onto an electrode.	Recovery of metal in metallic form.	High operating costs.
Electrodialysis	Membrane process driven by electric potential to remove heavy metal.	High recovery of water.	High operating costs. Heavy metal concentrate requires disposal.

1.1.3 Bioremediation and biorecovery of aqueous lead by local lead-resistant organisms

A promising alternative to conventional technology for the removal of aqueous Pb is bioremediation, where organisms are used to remove or detoxify the heavy metal (Philp et al., 2005). Bioremediation is attractive due to the variety of biomaterials applicable (such as algae, fungi, plants, and bacteria) and its potential for low cost and high efficiency operation at low Pb concentrations (Kang et al., 2015). Pb removal with organisms has mostly been limited to sorption with biomass (Chatterjee et al., 2012), the use of plants for phytoextraction (Shakoor et al., 2013), and fungi for mycelial biosorption (Chakraborty et al., 2013). Some microorganisms have been discovered that reduce the bioavailability and toxicity of Pb by precipitating it out as an insoluble complex. *Staphylococcus aureus*, for example, has been found to take up Pb(II) and precipitate it out as $Pb_{3n}(PO_4)_{2n}$ crystals (Levinson et al., 1996; Naik and Dubey, 2013). Additionally, several species of Pb-resistant marine bacteria tend to form insoluble PbS (De et al., 2008) when exposed to Pb(II).

Several subterranean anaerobic bacteria have been reported to respire using a range of terminal electron acceptors, including heavy metal pollutants (Haas et al., 2001). Respiration involving the reduction of soluble oxidised-metals can lessen the mobility of the metal.

A consortium of bacteria has been isolated from lead-contaminated soil at a battery recycling plant in Gauteng, South Africa, that has been shown to remove Pb(II) from solution (Brink, Lategan, et al., 2017). This lead-resistant consortium has been the subject of many investigations in the pursuit of better understanding the removal mechanisms and possible implementations in the bioremediation and biorecovery of lead in industrial effluent. This includes studies on the influence of lead concentrations (Brink, Lategan, et al., 2017; Peens, Wu, et al., 2018a), substrate concentration (Brink, Lategan, et al., 2017; Brink and Mahlangu, 2018), precipitate identification (Brink, Hörstmann, et al., 2019; Peens, 2018), and the influence of Zn(II) and Cu(II) concentrations (Hörstmann et al., 2020). Key findings in the investigations are outlined in this section.

Consortium characterisation

Streak and spread plates were prepared for the lead resistant culture at 80 and 500 mg L^{-1} Pb(II). The streak plate analyses was used to confirm the presence and abundance of species in the consortium using sequencing and analysis from the Basic Local Alignment Search Tool (BLAST). In the spread plates, colonies exhibiting precipitate formation were isolated before being sequenced and anal-

ysed using 16s rRNA genetic fingerprinting in order to identify dominant bacteria.

The streak plates showed that at 80 mg L^{-1} *Enterococcus* sp. and *Clostridium botulinum* were present in the largest quantity, but at 500 ppm Pb(II), *Ralstonia solanacearum* and *Klebsiella pneumoniae* were the most abundant. Furthermore, *Klebsiella pneumoniae* was identified as the dominant bacteria in spread plate isolates from both 80 and 500 mg L^{-1} (Peens, 2018).

Lead precipitation

Analysis revealed that PbS made up approximately 80 % of the precipitate formed when the culture was exposed to 80 mg L^{-1} Pb(II) and 40 % at 500 mg L^{-1} (Peens, 2018). A study into the minimum inhibitory Pb(II) concentration of the culture identified the precipitate ratio of PbS:Pb as 0.82:0.18 in batch processes, confirming the production of elemental lead by the consortium.

Modelling microbial kinetics

Hörstmann (2019) studied the kinetic behaviour of the consortium over 33 h and 15 d periods in batch reactors with varied substrate and Pb(II) initial concentrations. Kinetic models for Pb(II) removal and growth kinetics were developed.

The lead-removal model was formed on several assumptions based on experimental data, namely that growth and substrate concentration do not affect the removal rate and that removal occurs in separate fast and slow mechanisms. The model is presented in Equation 1.1:

$$-\frac{dC}{dt} = \left(\frac{k_m C}{C + K_c}\right)_{\text{fast}} + \left(\frac{k_m C}{C + K_c}\right)_{\text{slow}} \tag{1.1}$$

Where C is the concentration of Pb(II) in mg L^{-1}, t is time in d, k_m is the maximum reduction rate in mg L^{-1} d^{-1}, and K_c is the half-velocity constant in mg L^{-1}. The integrated form of Equation 1.1 is given in Equation 1.2:

$$C(t) = C_0 \left[\phi e^{\alpha_{\text{fast}}} + (1 - \phi)\, e^{\alpha_{\text{slow}}}\right] \tag{1.2}$$

Here, C_0 is the initial concentration of Pb(II) in mg L^{-1}, ϕ is the fraction of lead removal involved in the fast phase, and $\alpha = \frac{k_m}{K_c}$ for either the slow or fast phase. Parameters estimated for the kinetics of Pb(II) removal are given in Table 1.4.

A model for consortium growth was proposed based on metabolic activity readings. Metabolic activity was measured with 3-(4,5-dimethylthiazol-2-yl)-2,5-diphenyl tetrazolium bromide, or MTT. MTT is a yellow dye that is reduced

Table 1.4: Constants fit by Hörstmann (2019) for Equation 1.2.

ϕ	0.596
α_{fast}	17.39
α_{slow}	0.0436

to formazan crystals by the dehydrogenase system of viable Gram-negative bacterial cells. MTT is added to a reactor sample and incubated for an hour, after which formazan crystals are dissolved by dimethyl sulfoxide. A spectrophotometer with light at 550 nm is thereafter used to quantify the amount of light absorbed by formazan and infer metabolic activity.

Growth modelling was split into three consecutive phases, focusing on changes in biomass with dominant influences from nitrates, substrate, and the death of cells. These three factors are accounted for in Equation 1.3.

$$\frac{dX}{dt} = \left(\frac{dX}{dt}\right)_{\text{NO}_3} + \left(\frac{dX}{dt}\right)_{\text{subst}} + \left(\frac{dX}{dt}\right)_{\text{death}} \tag{1.3}$$

Where X is the biomass concentration in AU (absorbance units). The phase initially observed is nitrate dependent is modelled on Monod kinetics as:

$$\left(\frac{dX}{dt}\right)_{\text{NO}_3} = \left[\frac{\mu_{\max}}{1 + \frac{C}{K_i}}\right]\left(\frac{N - N_{\text{crit}}}{k_S + N - N_{\text{crit}}}\right) X \tag{1.4}$$

Here, $\mu_{\max}$ is the maximum specific growth rate in d^{-1}, K_i is the Pb(II) inhibition constant in mg L^{-1}, N is the concentration of $NO_3{}^-$ in g L^{-1}, N_{crit} is the critical concentration of $NO_3{}^-$ in g L^{-1}, and k_S is the half velocity constant in mg L^{-1}. Parameters estimated for the kinetics of nitrate dependant growth are given in Table 1.5.

Table 1.5: Constants fit by Hörstmann (2019) for Equation 1.4.

$\mu_{\max}$	$28.2\ \text{d}^{-1}$
k_s	$0.01\ \text{mg L}^{-1}$
K_i	$498.8\ \text{mg L}^{-1}$
N_{crit}	??

The relationship between nitrates and growth is also described in this phase as:

$$\frac{dX}{dt} = Y_{XN}\frac{dN}{dt} \tag{1.5}$$

Where Y_{XN} is the yield of biomass from nitrates in $\mathrm{AU \cdot L \cdot g^{-1}}$. Hörstmann (2019) found that at $C_0 = 500\,\mathrm{mg\,L^{-1}}$ then $Y_{XN} = 0.0487\,\mathrm{AU \cdot L \cdot g^{-1}}$, whereas at $C_0 = 80\,\mathrm{mg\,L^{-1}}$ then $Y_{XN} = 0.0110\,\mathrm{AU \cdot L \cdot g^{-1}}$.

A logistic differential model is used to describe the second phase of growth enhanced by substrate:

$$\left(\frac{dX}{dt}\right)_{\text{subst}} = \mu_{\max} X \left(\frac{K - X}{K}\right) \tag{1.6}$$

Where K is the biomass carrying capacity of the system in AU. Cultures grown with initial concentrations of $80\,\mathrm{mg\,L^{-1}}$ Pb(II) and $25\,\mathrm{g\,L^{-1}}$ substrate showed no substrate enhanced growth, whereas the parameters for cultures grown at double that initial substrate concentration and $500\,\mathrm{mg\,L^{-1}}$ Pb(II) are given in Table 1.6.

Table 1.6: Constants fit by Hörstmann (2019) for Equation 1.6 at initial conditions of $10\,\mathrm{g\,L^{-1}}$ yeast extract, $20\,\mathrm{g\,L^{-1}}$ tryptone, $1\,\mathrm{g\,L^{-1}}$ NaCl, and $500\,\mathrm{mg\,L^{-1}}$ Pb(II) at the start of enhanced growth phase.

X_0	8.27 AU
$\mu_{\max}$	$9.88\,\mathrm{d^{-1}}$
K	13.23 AU

The final phase in the model uses one-phase decay to describe the death of cells as:

$$\left(\frac{dX}{dt}\right)_{\text{death}} = -K_d X \tag{1.7}$$

With K_d being a constant in $\mathrm{d^{-1}}$. The parameters estimated for the death phase of two experimental runs are given in Table 1.7.

Table 1.7: Constants fit by Hörstmann (2019) for Equation 1.7 from the biomass concentration at the start of the death phase (X_{d0}) until equilibrium X_f.

C_0 ($\mathrm{mg\,L^{-1}}$)	Initial substrate ($\mathrm{g\,L^{-1}}$, excl. NaCl)	X_{d0} (AU)	X_f (AU)	K_d ($\mathrm{d^{-1}}$)
80	15	8.77	4.09	0.594
500	30	13.25	6.682	0.4136

Continuous reactor

Chimhundi et al. (2020) used the consortium in a continuous upflow anerobic sludge blanket reactor (CUASBR). The reactor demonstrated half the contact time necessary for lead reduction when compared to batch processes but only achieved 0.03 % lead recovery. New precipitates identified from the reactor include apatite and pyromorphite.

Shock loading in the CUASBR also demonstrated the ability of the consortium to survive at concentrations of 2000 mg L^{-1}.

1.2 The role of biosorption

The model presented in Equation 1.1 for the removal of Pb(II) does not distinguish between metabolically active processes of and the passive adsorption of lead onto cell walls. Literature, however, suggests that the fast phase in Equation 1.1 could be attributed to a rapid initial phase of biosorption. This is backed up by findings such as Pb(II) adsorption onto yeast reaching equilibrium after 6 minutes (Duncan et al., 2003), 95 % Pb(II) removal after 60 seconds by the algae *Spirulina* sp. (Van Hille et al., 2003), and Cu(II) adsorption reaching equilibrium in 30 minutes (Lawrence et al., 1985). This section discusses biosorption and its possible role in Pb(II) removal by the battery recycling plant consortium.

(Qin et al., 2020) Existing research shows that heavy metal removal takes place in two steps. The first step is metaolically independent and takes place on the surface of the cell, can also be done by dead bacteria. Physi, IX, and Surfcomplex.. Second phase involves surface microprecipitation and internal accumulation which require celluar energy

1.2.1 Introduction

In waste water treatment, adsorption describes a mass transfer process whereby pollutants are transferred from out of the liquid phase onto a solid surface (Wang and Guo, 2020). It is widely regarded as one of the most effective forms of advanced waste water treatment (Kumar Reddy and Lee, 2012), and is generally seen as both simple to implement and cost effective (Fomina and Gadd, 2014).

Biosorption is an umbrella term involving physico-chemical adsorption mechanisms to materials of biological origin (Robalds et al., 2016). Authors usually use the term exclusively for metabolically independent processes (Fomina and Gadd, 2014), in contrast to the non-passive mechanisms involved with bioaccumulation. The key biosorption terminology encountered in literature

and used in this dissertation is summarised in Figure 1.1. Sorption terms prefixed with *bio-* are frequently used interchangeably with terms prefixed with *ad-* within the confines of biosorption discussions.

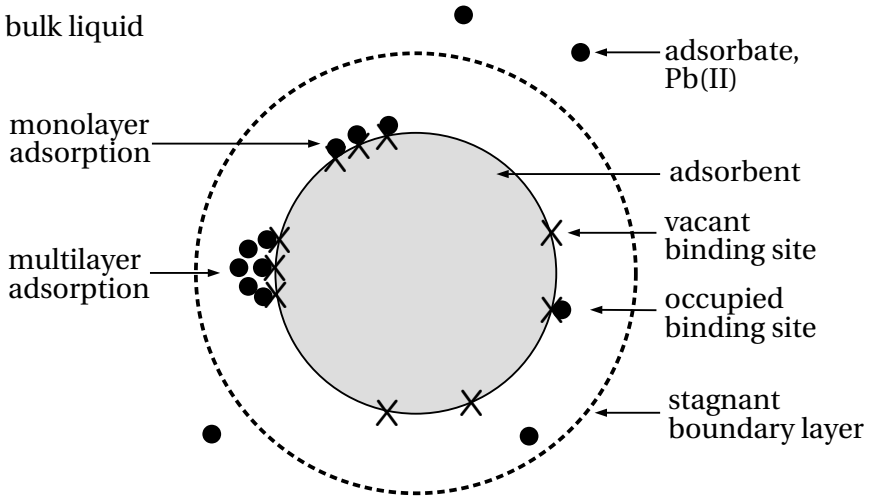

Figure 1.1: Visualisation of basic adsorption terminology. Adapted from Tran et al. (2017)

Adsorbents are primarily evaluated by how much adsorbate is retained by the material. This referred to as the uptake or adsorption capacity, and is calculated as (Volesky, 2007):

$$q = \frac{(C_0 - C)\,V}{W} \tag{1.8}$$

Where q is the adsorption capacity in $\mathrm{mg\,L^{-1}}$, V is the volume of adsorbate-bearing solution in L, and W is the dry mass of adsorbent in mg. The lead uptake calculated for a variety species of bacteria found in literature is given in Table 1.8.

1.2.2 Characteristising the consortium as a biosorbent

The characterisation of adsorbent properties forms a significant part in the study of new materials and can contribute greatly to the understanding and optimisation of biosorbents.

Table 1.8: Biosorption capacity of Pb(II) onto various species of bacteria.

Species	Pb(II) uptake ($mg\,g^{-1}$)	Reference
Acinetobacter junii L. Pb1	165	Kushwaha et al. (2017)
Arthrobacter sp.	130	Veglió et al. (1997)
Bacillus sp. (ATS-1)	92.3	Tunali et al. (2006)
Bacillus sp. PZ-1	9.30	Ren et al. (2015)
Bacillus firmus[a]	1100	Salehizadeh and Shojaosadati (2003)
Corynebacterium glutamicum	568	Choi and Yun (2004)
Curtobacterium sp. FM01	187	Masoumi et al. (2016)
Enterobacter sp. J1	50.0	Lu, Shi, et al. (2006)
Enterobacter cloacae	2.30	Ayangbenro and Babalola (2017)
Micrococcus luteus DE2008[b]	1965	Puyen et al. (2012)
Pseudomonas sp. LKS06	77.8	Huang and Liu (2013)
Pseudomonas aeruginosa PU21	0.735	Lin and Lai (2006)
Pseudomonas aeruginosa	110	Chang, Law, et al. (1997)
Pseudomonas putida	270	Uslu and Tanyol (2006)
Rhodococcus sp. HX-2	188	Hu et al. (2020)
Rhodococcus sp. HX-2 [c]	89.6	Hu et al. (2020)
Streptomyces rimosus [c]	135	Selatnia et al. (2004)

[a] Polysaccharide extract
[b] Living cells
[c] NaOH treated

Structure of bacteria

Most bacteria range in size from 1 to 10 µm and share several features highlighted in Figure 1.2. The interior of the cell consists of a semi-fluid medium, surrounded by a plasma membrane. The cell wall forms a secondary layer around this membrane, and in some bacteria this is enveloped by a gelatinous sheath referred to as the capsule (Mader, 1998).

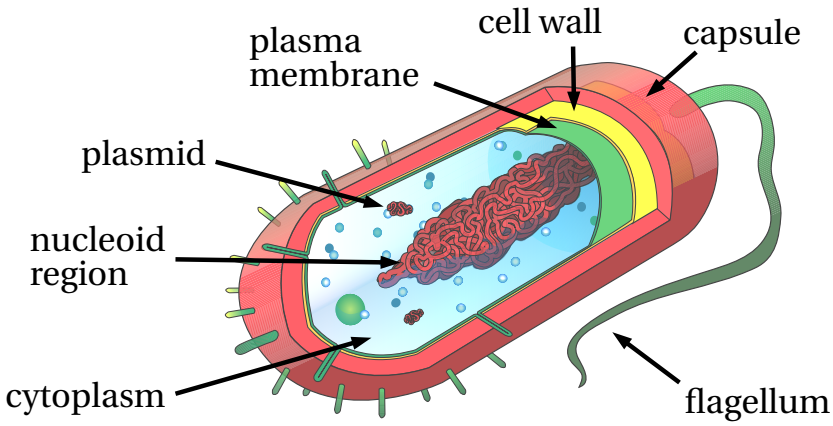

Figure 1.2: Basic structure of bacteria cell. Adapted from Villarreal (2008) and Mader (1998).

Bacteria are morphologically diverse and can appear spherical, rod-shaped, spiralled or filamentous (Wang and Chen, 2009). Cell wall structure varies greatly among bacteria, with two major divisions being species with Gram-positive or Gram-negative walls (Rosenberg et al., 2013). Both types have been identified in the battery recycling plant consortium: *Enterococcus* and *Clostridium* species are classified as Gram-positive, whereas *Klebsiella* and *Ralstonia* species are Gram-negative (Hörstmann, 2019; Peens, 2018).

Gram-positive bacteria have a 20 to 80 nm thick peptidoglycan (Figure 1.3) layer connected by amino acids and makes up 40 to 90 % of the cell wall (Wang and Chen, 2009). Teichoic acids link peptidoglycan to the plasma membrane. Functional groups within these two molecules as well as teichuronic acids contribute to an overall negative charge that facilitates the binding of metals (Vijayaraghavan and Yun, 2008).

Gram-negative cell walls have significantly less peptidoglycan (10 to 20 % composition) sandwiched between the plasma membrane and an outer membrane made up primarily of phospholipids and lipopolysaccharides (Vijayaraghavan and Yun, 2008). Figure 1.4 presents a typical lipopolysaccharide. The func-

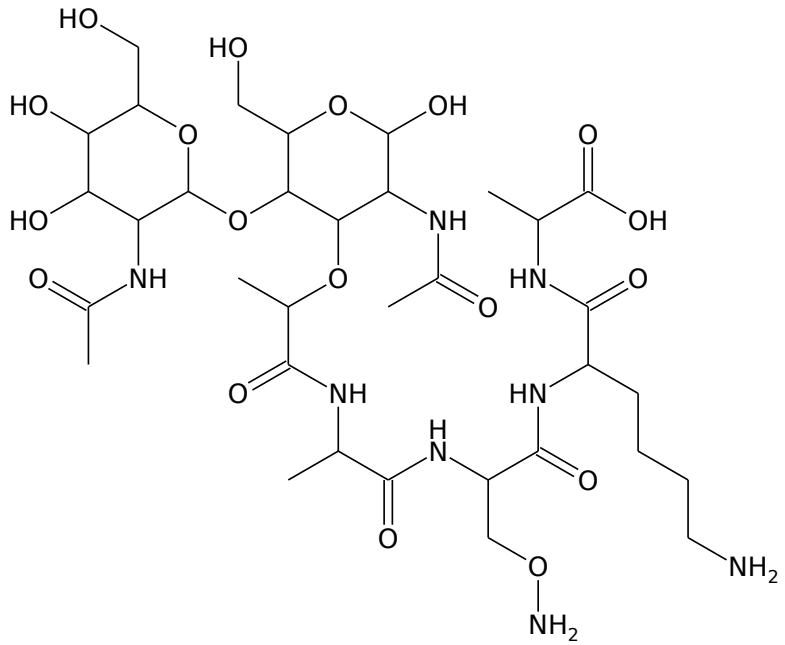

Figure 1.3: Peptidoglycan monomer. Adapted from the National Center for Biotechnology Information (2020b).

tional groups in peptidoglycan, phospholipids and lipopolysaccharides are responsible for the anionic character of the cell wall (Vijayaraghavan and Yun, 2008).

Extracellular polymeric substances (EPS) are also secreted on the surfaces of some bacteria and consist of proteins, polysaccharides, humic substances and nucleic acids (Zhang et al., 2017) that serve as both a protective layer and energy reserve for the cell (Liu and Fang, 2002). These substances have been found to contain significant amounts of negatively charged functional groups (Wang, Li, et al., 2014). Biofilms, capsules, slimes, and sheaths are composed of EPS and have been shown to contribute significantly to biosorption (Fomina and Gadd, 2014).

Laboratory characterisation

A variety of standard techniques are available for investigating and characterising the basic properties of an adsorbent. Unuabonah et al. (2019) stresses the importance of accurate characterisation for the purposes of maximising adsorbent use in batch and continuous systems. Table 1.9 outlines methods commonly used for determining adsorbent characteristics.

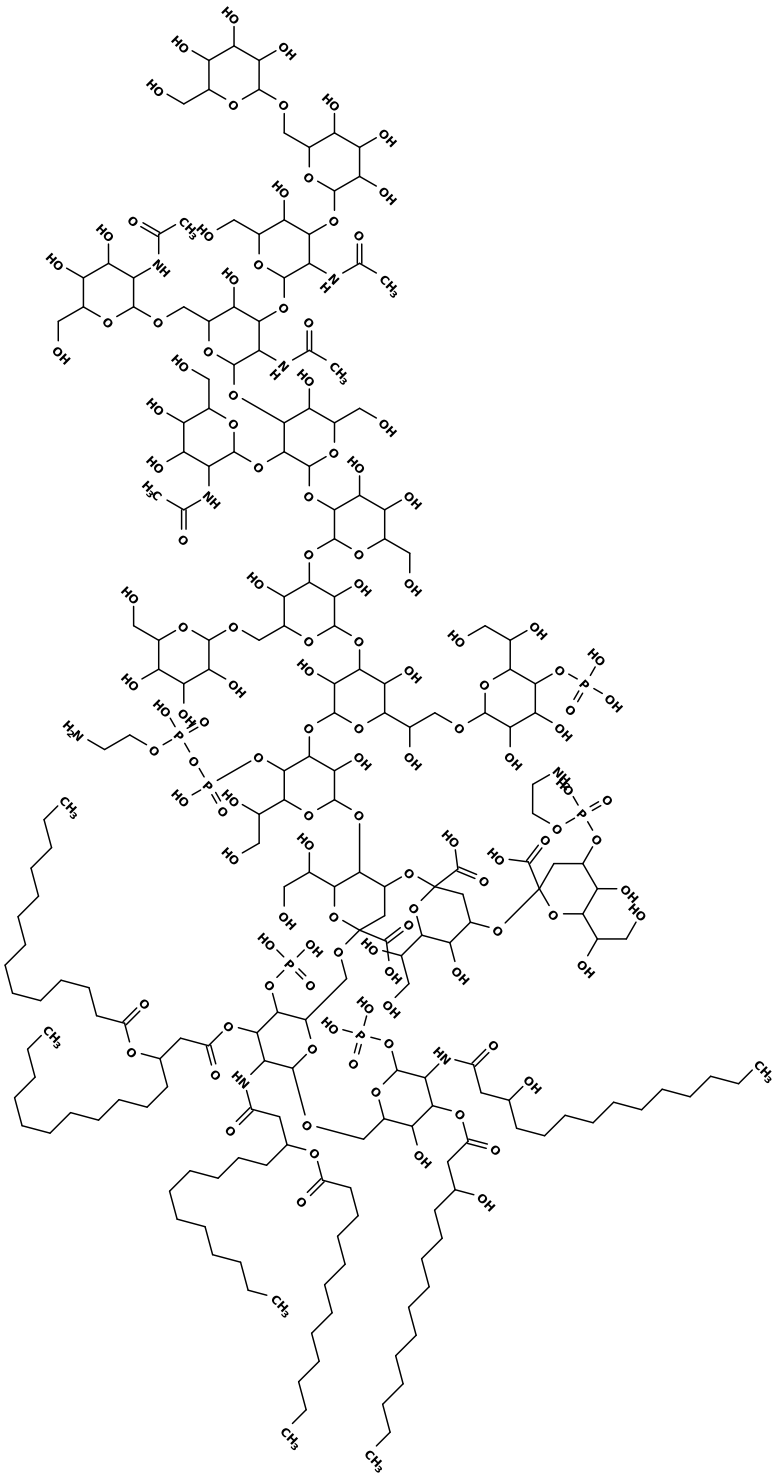

Figure 1.4: Example of a lipopolysaccharide molecule typically found in species like *Escherichia coli* (Whitman, 2010). Adapted from National Center for Biotechnology Information (2020a).

Table 1.9: Techniques employed for determining various adsorbent properties. Adapted from Tran et al. (2017)

Property	Technique	Description
Surface chemistry	Energy dispersive X-ray spectroscopy (EDS)	Samples are exposed to beam of X-rays, allowing elements to be identified as they excite and emit unique fluorescence X-rays.
	Fourier transform infrared spectroscopy (FTIR)	The amount of infrared light absorbed in a sample by molecular bonds is used to infer what bonds are present and how biosorption alters these bonds.
	Raman spectroscopy (RS)	Visible or infrared light is is passed through a sample. The amount of light scattered can be used to identify molecular bonds.
	Potentiometric titration	Point of zero charge (pH_{pzc}) determined where there is an absence of adsorbent surface charge.
	Electrophoresis	An electric field is applied in combination with light scattering to determine the zeta potential, defined as the potential difference at the interface of the diffusion layer of the adsorbent and bulk fluid used as a measure of electrostatic repulsion.
Morphology	Scanning electron microscopy (SEM)	An electron beam scans across the adsorbent surface, resulting in scattered electrons that are used to generate an image.
	Transmission electron microscope (TEM)	A high powered beams of electrons is sent through a cross section of a sample, resulting in interactions with the sample that are used to generate an image.
	Laser diffraction	Samples are exposed to a laser beam. The patterns of diffraction are analysed and used to infer particle size.

Table 1.9: Techniques employed for determining various adsorbent properties. Adapted from Tran et al. (2017)

Property	Technique	Description
Hydrophobicity	Water contact angle	The shape of the liquid-vapour interface of water on the sample is used to determine surface wettability.
Textural property	BET specific surface area	The volume of N_2 adsorbed on the adsorbent surface can be used to infer surface are.
Thermal stability	Thermal gravimetric analysis	The mass of a sample is recorded as a function of temperature and time to quantitatively analyse composition.
Crystalline structure	X-ray diffraction	The diffraction pattern that arises from a sample being exposed to an X-ray beam is used to identify crystalline compounds.
Proximate analysis	ASTM international standards	A variety of standardised methods employed to determine the distribution of major constituents.
Ultimate analysis	ASTM international standards	A variety of standardised methods employed to determine the distribution of carbon, hydrogen, oxygen and nitrogen.
Adsorption of substance	Iodine number	The mass of iodine consumed by the adsorbent is used to compare adsorption surface area and porosity.
	Molasses number	The measure of the amount of colour removed from molasses by an adsorbent and is used to evaluate the macro pore structure.
	Methylene blue index	The measure of the amount of methylene blue adsorbed by a sample for the purpose of determining the cationic exchange capacity.

1.2.3 Mechanisms of metal biosorption

Biosorption mechanisms are highly complex and can involve multiple, simultaneous reactions that contribute to differing degrees (Fomina and Gadd, 2014). Figure 1.5 gives an overview of the mechanisms involved in biosorption within the context of sorption as a whole. However, the hierarchical arrangement of mechanisms differs among authors (Robalds et al., 2016). The extent to which each mechanism is involved varies significantly and is dependent on the adsorbate, ionic strength of solution and the chemical nature of the adsorbent (Yang, Wan, et al., 2019).

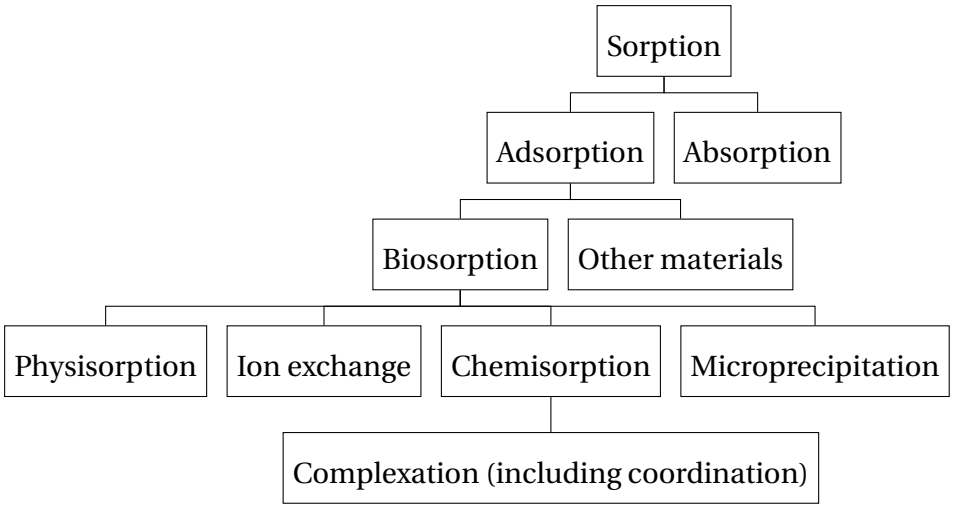

Figure 1.5: Classification sorption mechanisms as proposed by Robalds et al. (2016)

Physisorption Physical adsorption of ions onto biomass is primarily caused by van der Waals and electrostatic forces (Suzuki, 1990). Due to the ionisation of functional groups, most biosorbents have been found to have net negative surface charges (Farhan and Khadom, 2015) that assist in the attraction of positive metal ions towards the adsorbent (Hammaini et al., 2007).

Ion exchange Light metal ion exchange involves several adsorption mechanisms where the cations Ca^{2+}, Mg^{2+}, K^{+}, and Na^{+} are released from the biomass surface and replaced by a heavy metal. Table 1.10 shows the molar ratio of Pb^{2+} bound by adsorption to cations released as a result of adsorption, $R_{b/r}$. If $R_{b/r} \leq 1$, then ion exchange is a prominent mechanism of adsorption. On the contrary, if $R_{b/r} \geq 1$, then other mechanisms would dominate heavy metal

adsorption (Saha et al., 2017). It has also been reported that high concentrations of light earth metals tend to compete with heavy metals for adsorption sites adsorption (Xu et al., 2013).

Table 1.10: Contribution of cation exchange to Pb^{2+} adsorption

Biosorbent	Cations released	$R_{b/r}$ (mol Pb^{2+}/mol cation)	Reference
Sludge derived biochar	Mg^{2+}, Ca^{2+}, K^+, Na^+	0.768	Lu, Zhang, et al. (2012)
Colocasiaesculenta(L.) Schott	Ca^{2+}, K^+	0.12	Saha et al. (2017)
Agaricus bisporus	Mg^{2+}, Ca^{2+}, K^+	0.9382	Xu et al. (2013)

Chemisortption Functional group complexation is a category of adsorption mechanisms whereby ligands act as binding sites by donating electron density to metal ions (Kotz et al., 2014; Smith, 2014). This mechanism is initiated by the deprotonation of a ligand, as illustrated for divalent metals in Equation 1.9, Equation 1.10 and Equation 1.11.

$$LH \longrightarrow L^- + H^+ \tag{1.9}$$

$$L^- + M^{2+} \longrightarrow LM^+ \tag{1.10}$$

$$2\,L^- + M^{2+} \longrightarrow 2\,LM \tag{1.11}$$

Here, L represents functional groups that act as ligands and M represents the metal. Functional group complexation can be a prominent adsorption mechanism for some bacteria that use it to concentrate terminal electron accepting ions on the cell wall surface (Haas et al., 2001). The functional groups most prominently involved adsorption include hydroxyl and carboxyl groups (Lu, Zhang, et al., 2012; Chen, Liu, et al., 2014; Costa et al., 2010; Fomina and Gadd, 2014). Biomass typically contains an abundance of these groups, as seen in Figure 1.3 and Figure 1.4. Other functional groups like phosphate, amine, carbonyl, and ether also play a role (Fein et al., 1997; Mathew and Krishnamurthy, 2018; Chen and Yang, 2006). The interaction between functional groups and

aqueous metals involves a variety of arrangements that make modelling complexation problematic (Chen and Yang, 2006), as demonstrated in Figure 1.6 and Figure 1.7 for carboxyl groups.

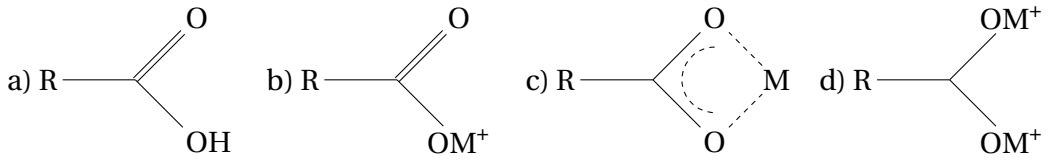

Figure 1.6: Possible inner-sphere functional group complexation with a divalent metal M^{2+} and carboxyl groups, with a) being protonated before complexation, b) unidentate complexation, c) bindentate complexation, and d) bridging. Adapted from Chen and Yang (2006).

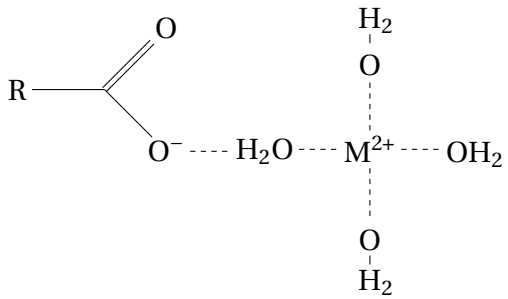

Figure 1.7: Possible outer-sphere complexation with divalent metal M^{2+} and a carboxyl group. Adapted from Worch (2012).

(Ngwenya and Chirwa, 2015)

Due to the role of deprotonation, solution pH has a large impact on functional group complexation (Lee et al., 1999; Chen, Liu, et al., 2014; Worch, 2012). At lower pH values, H^+ ions compete with metals for adsorption sites (Hammaini et al., 2007) while at higher pH values divalent metals form aqueous hydroxide species (Grivé et al., 2010). Optimal pH values between 4 and 6 frequently reported in biosorbent studies (Duncan et al., 2003; Chen and Yang, 2006; Costa et al., 2010; Guiza, 2017; Hammaini et al., 2007; Lu, Zhang, et al., 2012).

The role of outer sphere complexation can be investigated by experimentation, since it is more sensitive to variations in ionic strength than inner sphere complexation (Ngwenya and Chirwa, 2015).The extent to which each functional group participates in biosorption can also be investigated by experiment. Esterification of hydroxyl and carboxyl groups by acidic methanol, for example, is capable of blocking the complexation of these functional groups. This process

has been found to reduce Pb(II) biosorption by up to 38 % in apple residue (Lee et al., 1999) and up to 42 % in sludge derived biochar (Lu, Zhang, et al., 2012).

Potentiometric titration is also used to determine the equilibrium constants and concentration of various functional groups (Turner, 2005), while Boehm titrations can be used to identify and quantify carboxylic, lactonic, and phenolic functional groups (Seung Kim and Rae Park, 2016).

Microprecipitation The surface precipitation of Pb(II) generally involves reactions with phosphate to form pyromorphite and hydropyromorphite (Li et al., 2017).

1.2.4 Modelling batch adsorption

The employment of biosorption models prove useful in gaining an understanding of adsorbent capacity, the mechanisms of adsorption, the influence of operating conditions, equilibrium behaviour and optimisation possibilities (Anastopoulos and Kyzas, 2015; Unuabonah et al., 2019). Modelling the process of biosorption has been undertaken using several approaches that are grouped as either empirical (equilibrium and kinetic) or mechanistic (Chen and Yang, 2006).

Empirical models are not computationally intensive, and, as the name suggests are more focused on predicting the outcome of experimental results based on limited adjustable parameters (Vijayaraghavan and Yun, 2008). Almost all empirical models are fit only for specific temperature and pH operating conditions, although some authors have modified existing adsorption models to predict the effect of pH or temperature (Esposito et al., 2002; Jeppu and Clement, 2012). The kinetic and equilibrium empirical models presented in this dissertation were not derived for biosorption nor do many of their assumptions apply, yet they have been shown as capable of reflecting biosorption experiments (Vijayaraghavan and Yun, 2008).

Equilibrium models

Several empirical equilibrium models are given in Table 1.11.

Mechanistic models are based on the knowledge of binding sites from biomass characterisation and the associated adsorption reactions (Vijayaraghavan and Yun, 2008). These models are used less often than empirical counterparts but are more valuable for explaining the outcome of experiments (Unuabonah et al., 2019). The models presented in this section deal with describing surface complexation mechanism.

The following equilibrium equations can be used to describe acid-base chemistry and unidentate surface complexation at an oxidic binding site (Ngwenya, Sutherland, et al., 2003; Stumm, 1992):

$$\mathrm{R{-}OH^{0+}} \rightleftharpoons \mathrm{R{-}O^{-}} + \mathrm{H^{+}} \qquad K_1 = \frac{\{\mathrm{R{-}O^{-}}\} a_{\mathrm{H}}}{\{\mathrm{R{-}OH^{0}}\}} \tag{1.12}$$

$$\mathrm{R{-}OH_2^{+}} \rightleftharpoons \mathrm{R{-}OH^{0}} + \mathrm{H^{+}} \qquad K_2 = \frac{\{\mathrm{R{-}OH^{0-}}\} a_{\mathrm{H}}}{\{\mathrm{R{-}OH_2^{+}}\}} \tag{1.13}$$

$$\mathrm{R{-}O^{-}} + \mathrm{M}^{m+} \rightleftharpoons \mathrm{R{-}OM}^{m-1} \qquad K_M = \frac{\{\mathrm{R{-}OM}^{m-1}\}}{\{\mathrm{R{-}O^{-}}\}\, a_{\mathrm{M}}} \tag{1.14}$$

where R represents the cell wall, M^{m+} represents a metal ion of valence m, and a_i is the activity the species i. The notation $\{\}$ denotes concentration in mol g^{-1} adsorbent, and can be converted to units of mol L^{-1} solution through multiplication with adsorbent concentration. The total metal concentration is defined as:

$$[\mathrm{M}]_{\mathrm{tot}} = [\mathrm{M}^{m+}] + [\mathrm{R{-}OM}^{m-1}] \tag{1.15}$$

Furthermore, the total number of sites can be found from the mass balance:

$$\{\mathrm{R{-}O}\}_{\mathrm{tot}} = \{\mathrm{R{-}O^{-}}\} + \{\mathrm{R{-}OH^{0}}\} + \{\mathrm{R{-}OH_2^{+}}\} + \{\mathrm{R{-}OM}^{m-1}\} \tag{1.16}$$

Activity can be calculated using the Davies equation (Turner, 2005) as

$$a_i = c_i \gamma_i \tag{1.17}$$

$$\log(\gamma_i) = -0.5092 z^2 \left(\frac{\sqrt{I}}{1+\sqrt{I}} - 0.3I \right) \tag{1.18}$$

where c_i is molar concentration in mol L^{-1}, γ_i is the activity coefficient, z is the ion valence, and I is the ionic strength in mol L^{-1}.

The surface charge introduced by functional groups on adsorbents produces an electric field that interacts with aqueous ions. This influence on the equilibrium constant K_n for reaction n can be described as follows (Fein et al., 1997):

$$K_n = K_{n,\,\mathrm{int}} \exp\left(-\frac{\Delta z F \psi}{RT} \right) \tag{1.19}$$

where $K_{n,\,\mathrm{int}}$ is the equilibrium constant for reaction n when no surface charge is present, Δz is the change in valence for the surface species, F is the Faraday constant (96 485 C mol^{-1}), ψ is the surface potential in V, R is the gas constant in J mol^{-1} K^{-1} and T is the temperature in K.

Several models have been developed for calculating ψ as a function of surface charge density to determine the influence of electrostatic effects on K_n. Surface charge density is generally calculated using the sum of charged sites

$$\sigma = F \sum_j \left(\frac{\{\text{R–O}^-{}_j\} + \{\text{R–OH}_2{}^+{}_j\}}{A_m} \right) \tag{1.20}$$

where j is a specific functional group, σ is surface charge density in C m^{-2}, A_m is the specific surface area in $\text{m}^2\,\text{g}^{-1}$. Potentiometric titration experiments can also be used to determine σ:

$$\sigma = \frac{Q_s F}{A_m} \tag{1.21}$$

$$Q_s = \frac{V}{W} \left(c_a - c_b - \log(\text{pH}) + \log(\text{pOH}) \right) \tag{1.22}$$

Here, Q_s is the surface charge calculated from titration in mol g^{-1} adsorbent, V is the volume of adsorbate-bearing solution in L, W is the dry mass of adsorbent in mg, and c is the concentration in mol L^{-1} of acid a or base b added during titration.

Four of models used to describe the effect of σ on ψ are discussed in this section.

Non-electrostatic adsorption In order to simplify surface complexation modelling, $K_n = K_{n,\,\text{int}}$ is assumed in the non-electrostatic adsorption model (NEM) (Turner, 2005). Esposito et al. (2002) employed a simple mechanistic NEM for modelling heavy metal adsorption onto the bacteria *Sphaerotilus natans*. The model assumes an ideal solution, negligible electrostatic effects, a non-competitive mechanism and only one type of binding site. The assumptions result in the following relationships:

$$K_1 = K_{1,\,\text{int}} \tag{1.23}$$

$$K_M = K_{M,\,\text{int}} \tag{1.24}$$

$$\{\text{R–OM}^{m-1}\} = \frac{q_e}{M_{\text{M}}} \tag{1.25}$$

$$a_{\text{M}} = [\text{M}^{m+}] = c_e \tag{1.26}$$

$$a_{\text{H}} = [\text{H}^+] = 10^{-\text{pH}} \tag{1.27}$$

Where M_{M} is the molar mass of metal M. These equations can be combined with the equilibrium constants of Equation 1.12 and Equation 1.14 as well as the mass balance of Equation 1.16 to derive the isothermal profile:

$$q_e = \frac{c_e M_{\text{M}} \{\text{R–O}\}_{\text{tot}}}{\left(1 + 10^{-\text{pH}}/K_1\right)\,(K_M + c_e)} \tag{1.28}$$

Constant capacitance The constant capacitance model is used under the assumption that only inner-sphere complexes form, no surface complexes are formed with ions from the background electrolyte, and that the suface has only one plane of charge (Goldberg, 1995). The surface potential ψ is determined with the expression (Ngwenya, Sutherland, et al., 2003)

$$\psi = \frac{\sigma}{C} \tag{1.29}$$

C is capacitance density in $\mathrm{F\,m^{-2}}$. Fein et al. (1997) found that a C of $8.0\,\mathrm{F\,m^{-2}}$ best fit titration data for *Bacillus subtilis*. Other authors have subsequently made use of this capacitance density for modelling *Pantoea agglomerans* (Ngwenya, Mosselmans, et al., 2009), *Escherichia coli* (Chang, Brewer, et al., 2020), and a culture sourced from diesel contaminated soil (Ngwenya, Sutherland, et al., 2003). Parameter optimisation is, however, relatively insensitive to the chosen value of C (Lützenkirchen, 1999).

Double layer The double, diffuse, or diffuse double layer model has the same assumptions as the constant capacitance model with the exception of having two planes of charge (Goldberg, 1995). The relationship between surface potential and surface charge density is described as (Turner, 2005)

$$\psi = \frac{2RT}{zF} \sinh^{-1}\left(\frac{\sigma}{\sqrt{8RT\epsilon\epsilon_0 c}}\right) \tag{1.30}$$

Here, z is the counter ion valence, c is the concentration of the counter ion in $\mathrm{mol\,L^{-1}}$, ϵ is the dielectric constant of water (78.5), and ϵ_0 is the permittivity in vacuum ($8.854 \times 10^{-12}\,\mathrm{C\,V^{-1}\,m^{-1}}$) (Huang and Wang, 2014).

Donnan shell Ohshima and Kondo (1990) remark that the double layer model is only accurate for ion-impenetrable surfaces and should not be applied to cell walls as a result. A more suitable complexation model is therefore given as (Ohshima and Kondo, 1990; Turner, 2005):

$$\psi_{\mathrm{DON}} = \frac{RT}{zF} \sinh^{-1}\left(\frac{\sigma_s}{2zFc}\right) \tag{1.31}$$

$$\psi = \psi_{\mathrm{DON}} - \frac{RT}{zF} \tanh\left(\frac{zF\psi_{\mathrm{DON}}}{2RT}\right) \tag{1.32}$$

where ψ_{DON} is the Donnan potential in V. This model differs from the double layer and constant capacity models in that volume charge density (σ_s in $\mathrm{C\,m^{-3}}$)

is used instead of σ. This is calculated as

$$\sigma_s = F \sum_j \left(\frac{\{\text{R}-\text{O}^-{}_j\} + \{\text{R}-\text{OH}_2{}^+{}_j\}}{V_m} \right) \tag{1.33}$$

Here, V_m is the specific volume of the adsorbent shell or the Donnan volume in $m^3\ g^{-1}$. Yee et al. (2004) calculates V_m using a dry cell density of 6.7×10^{12} cell g^{-1} and cell wall volume of 1.12 μm^3 cell^{-1} for *Bacillus subtilis*. The cell wall volume was calculated on the basis of a cell wall thickness of 25 nm and cylindrical cell geometry with dimensions of 1×5 µm, although Yee et al. (2004) caution that cell wall charge is highly sensitive to cell dimension and density estimates.

More complicated mechanistic models have been developed to factor in multiple types of binding sites (Pagnanelli et al., 2005), metal hydrolysis equilibria (Yang and Volesky, 1999; Haas et al., 2001; Dai et al., 2010) and the influence of alkaline earth metal concentration (Chen and Yang, 2006). These additional factors often require further experimentation and solving of multiple, complex non-linear equations which limit their implementation (Vijayaraghavan and Yun, 2008).

Thermodynamics Many authors make use of adsorption isotherms at multiple temperatures to investigate the spontaneity, randomness and the exothermic or endothermic nature of biosorption (Rangabhashiyam and Balasubramanian, 2019). Equation 1.34 and Equation 1.35 are used for this purpose:

$$\Delta G^\circ = -RT \ln K_C \tag{1.34}$$

$$\ln K_C = \frac{-\Delta H^\circ}{RT} + \frac{\Delta S^\circ}{R} \tag{1.35}$$

where ΔG° is the change in Gibbs free energy (J mol^{-1}), ΔH° is the change in enthalpy (J mol^{-1}) and ΔS° is the change in entropy (J mol^{-1} K^{-1}). T is the temperature (K), R is the universal gas constant, and K_C is the distribution coefficient calculated as $K_C = q_e/C_e$.

Table 1.11: Empirical equilibrium adsorption models

Model	Description	Equation	Description of equation
Langmuir	The Langmuir adsorption isotherm model is the most frequently encountered equilibrium model in literature. It was originally developed for the adsorption of gases onto surfaces and is used under the assumption that there is a fixed number of homogeneous sites where reversible, monolayer adsorption takes place with no interaction between adsorbate species (Langmuir, 1918).	$q_e = \frac{q_{\max} K_L C_e}{1 + K_L C_e}$ (1.36)	q_e is the equilibrium adsorption capacity ($\mathrm{mg\,g^{-1}}$), $q_{\max}$ is the maximum adsorption capacity ($\mathrm{mg\,g^{-1}}$), K_L is the Langmuir adsorption equilibrium constant ($\mathrm{L\,mg^{-1}}$) related to affinity between adsorbate and adsorbent, and C_e is the equilibrium concentration of adsorbate in solution ($\mathrm{mg\,L^{-1}}$). Heterogeneous adsorption can be modelled with the sum of multiple homogeneous isotherms (Langmuir, 1918).
Modified Langmuir	Esposito et al. (2002) proposed a modification for Equation 1.36 that describes the effect of pH on $q_{\max}$.	$q_{\max} = \frac{q_0 e^{k_E \mathrm{pH}}}{1 - \frac{q_0}{q_\infty}\left(1 - e^{k_E \mathrm{pH}}\right)}$ (1.37)	q_0, q_∞, and k_E are adjustable constants.
Freundlich	The Freundlich isotherm equation describes reversible, non-ideal, multilayer adsorption and is usually used for heterogenous adsorbents like biomass (Foo and Hameed, 2010). This model has, however, been found to inadequately describe the linearity range at very low concentrations or saturation effects at very high concentrations (Tran et al., 2017).	$q_e = K_F C_e^{\alpha}$ (1.38)	K_F is the Freundlich constant in $(\mathrm{mg\,g^{-1}})(\mathrm{mg\,L^{-1}})^{-\alpha}$ and α is the Freundlich intensity parameter. The isotherm is linear when $\alpha = 1$, favourable when $\alpha \leq 1$, and unfavourable when $\alpha \geq 1$ (Tran et al., 2017). In addition, it has been reported that a value for α between 0 and 1 indicate surface heterogeneity, with more heterogeneous surfaces having values closer to 0 (Foo and Hameed, 2010).
Sips	The Sips isotherm, also referred to as the Langmuir-Freundlich model (Jeppu and Clement, 2012), is a three parameter power function based the assumption of continuously distributed affinity coefficients (Bolster and Hornberger, 2007). The Sips isotherm has been found to predict adsorption involving the occupation of two sites by a single adsorbent (Chan et al., 2012).	$q_e = \frac{q_{\max} K_S C_e^s}{1 + K_S C_e^s}$ (1.39)	K_S is the Sips constant in $(\mathrm{L/mg})^s$ and s is a fitting parameter between 0 and 1. Similar to the Freundlich model, this isotherm is appropriate for heterogeneous surfaces. At high adsorbate concentrations the model reduces to the Langmuir isotherm (Equation 1.36) and at low concentrations it resembles multilayer adsorption found in the Freundlich isotherm (Ayawei et al., 2017).

Table 1.11: Empirical equilibrium adsorption models

Model	Description	Equation	Description of equation
Modified Sips	Jeppu and Clement (2012) proposed a modification for Equation 1.39 to account for the effect of pH on K_S.	$\log K_S = M_1 \text{pH} + M_2$ (1.40)	M_1 and M_2 are constants.
Redlich-Peterson	The Redlich-Peterson model is also described as a hybrid between the Langmuir and Freundlich isotherms (Ayawei et al., 2017). This isotherm follows multilayer adsorption (Chan et al., 2012) and does not have good asymptotic behaviour for high adsorbate concentrations (Brouers and Al-Musawi, 2015).	$q_e = \frac{K_{RP} C_e}{1 + a_{RP} C_e^r}$ (1.41)	K_{RP} is a constant (L g^{-1}), a_{RP} is a constant $(\text{L mg}^{-1})^{-r}$ and r is a parameter with values constrained between 0 and 1. When $r = 1$, then Equation 1.41 reduces to the Langmuir isotherm (Equation 1.36). At high concentrations of adsorbate, the Redlich-Peterson model reduces to the Freundlich isotherm (Equation 1.38). When $r = 0$, Equation 1.41 reduces to Henry's law (Ayawei et al., 2017).
Temkin	The Temkin adsorption isotherm focuses on adsorbent-adsorbate interactions. The model assumes a uniform distribution of heterogeneous binding energies and a linear decrease in heat of adsorption (Dada et al., 2012).	$q_e = \frac{RT}{b_T} \ln (A_T C_e)$ (1.42)	A_T is the Temkin isotherm equilibrium binding constant (L g^{-1}), b_T is the Temkin isotherm constant (J mol^{-1}), and R is the universal gas constant of $8.314\ \text{J mol}^{-1}\ \text{K}^{-1}$.
Dubinin-Radushkevich	This model assumes a Gaussian energy distribution of heterogeneous sites (Inyinbor et al., 2016).	$q_e = q_{\max} e^{-K_{DR}\varepsilon^2}$ (1.43) $\varepsilon = RT \ln\left(1 + \frac{1}{C_e}\right)$ (1.44)	K_{DR} is the Dubinin-Radushkevich isotherm constant ($\text{mol}^2\ \text{J}^{-2}$).

Kinetic models

The modelling of time progress in adsorption can provide insight into the mechanism of sorption and behaviour leading up to equilibrium. Adsorption kinetics concerns four stages of transport (Worch, 2012):

1. Transport of adsorbate from bulk liquid phase to the stagnant boundary layer around the adsorbent.
2. External diffusion of adsorbate through the stagnant boundary layer to the adsorbent surface.
3. Internal or intraparticle diffusion of adsorbate.
4. Binding of adsorbate to final adsorption site.

Worch (2012) further states that these steps are modelled under the assumptions that temperature is constant, the bulk solution is completely mixed, and that the adsorbent particle is spherical and isotropic. In most cases the first and final steps are fastest, thereby leaving the external and internal mass transfer as the rate limiting steps. Internal mass transfer includes both surface and pore diffusion, where surface diffusion is generally assumed to be the dominant step (Worch, 2012). Several mass transfer and adsorbate binding models are given in this section, with empirical models presented in Table 1.12.

External diffusion Fick's law of diffusion can be used to model external mass transfer. However, this step is dependent on stirring speeds or flow rates and is almost never rate-limiting in experimental runs. As a result, it is generally not modelled by authors.

Internal diffusion Within a spherical adsorbent with a radius r (m) and effective adsorbate diffusivity D_e ($m^2\ s^{-1}$), internal mass transfer can be described in Equation 1.45 (Largitte and Pasquier, 2016):

$$\frac{\partial q}{\partial t} = \frac{D_e}{r^2}\frac{\partial}{\partial r}\left(\frac{r^2 \partial q}{\partial r}\right) \tag{1.45}$$

Here, t denotes time (min). Integrated solutions to Equation 1.45 are given by (Boyd et al., 1947) and (Reichenberg, 1953) in Table 1.12 as Equation 1.57 and Equation 1.58 respectively.

The Weber and Morris internal diffusion model is comparatively simpler and is also presented in Table 1.12 as Equation 1.59.

Final adsorption For the binding of an adsorbate to the final adsorption site, Langmuir kinetics consider the elementary reaction of metal M adsorbing onto site S as follows (Fogler, 2006):

$$\mathrm{M} + \mathrm{S} \rightleftharpoons \mathrm{MS} \tag{1.46}$$

The rate of adsorption r_a and the rate of desorption r_d is given in Equation 1.47 and Equation 1.48 respectively:

$$r_a = k_a C(1-\theta) \tag{1.47}$$
$$r_d = k_d \theta \tag{1.48}$$

Where k_a and k_d are rate rate constants for adsorption and desorption and θ is the fraction of adsorption sites covered ($0 \leq \theta \leq 1$). Therefore, the combined rate equation can be taken as:

$$\frac{d\theta}{dt} = r_a - r_d \tag{1.49}$$
$$\frac{d\theta}{dt} = k_a C(1-\theta) - k_d \theta \tag{1.50}$$

If the grams of solute adsorbed at any time can be represented as a fraction of the equilibrium adsorption q_e, i.e. $q = q_e\theta$, then Equation 1.50 can be rewritten as:

$$\frac{dq}{dt} = k_a C(q_e - q) - k_d q \tag{1.51}$$

Equation 1.51 is also referred to as the Adam-Bohart-Thomas model (Zhao, 2011). Defining $K_L = k_a/k_d$, Equation 1.51 reduces to the Langmuir isotherm (Equation 1.36) at equilibrium. The integrated solution of Equation 1.51 is given in Table 1.12 as Equation 1.61.

Pseudo-first- and pseudo-second-order models of kinetic adsorption have been developed and are also presented in Table 1.12. These models follow assumptions used to describe Langmuir adsorption (Largitte and Pasquier, 2016; Ho and McKay, 2000). Azizian (2004) showed that the pseudo-first- and pseudo-second-order models could be derived from Langmuir kinetics presented in Equation 1.50. When the initial concentration of adsorbate C_0 is very high, or the process modelled is still in initial adsorption phases, or when relatively few binding sites are present on the adsorbent, then pseudo-first-order kinetics approximate Langmuir kinetics. Similarly, it was shown that the pseudo-second-order model can be derived from Langmuir kinetics when C_0 is relatively low, adsorption is at the final stage, or if active sites are relatively abundant on the adsorbent (Wang and Guo, 2020).

Stumm (1992) presented a mechanistic approach to adsorption of divalent metal ions onto hydrous oxide surfaces. The process assumes attachment to the surface as an outer-sphere complex, followed by surface diffusion, metal complex dewatering, and finally the formation of a bond with the active site as follows:

$$\mathrm{R{-}OH} + \mathrm{M(H_2O)_n^{2+}} \overset{K_{OS}}{\rightleftharpoons} \mathrm{R{-}OH\cdots M(H_2O)_n^{2+}} \tag{1.52}$$

$$\mathrm{R{-}OH\cdots M(H_2O)_n^{2+}} \xrightarrow{k_{ads}} \mathrm{R{-}O(H)(M(H2O)_{n-1}^{2+})} + \mathrm{H_2O} \tag{1.53}$$

$$\mathrm{R{-}O(H)(M(H2O)_{n-1}^{2+})} \xrightarrow{k_{fast}} \mathrm{R{-}O{-}M(H_2O)_{n-1}^{+}} + \mathrm{H^+} \tag{1.54}$$

Here, K_{OS} is the outer-sphere surface complex formation constant and is calculated as:

$$K_{OS} = \exp\left(-\frac{Z\psi}{RT}\right) \tag{1.55}$$

Additionally, k_{ads} is the intrinsic adsorption rate constant at zero surface charge. The magnitude of this constant is largely dependent on the rate of dewatering from the metal held in the outer-sphere complex (Equation 1.53). Assuming $k_{fast} >> k_{ads}$, the surface complex rate of formation is calculated as:

$$\frac{d[\mathrm{R{-}OM^+}]}{dt} = K_{OS} k_{ads} [\mathrm{M^{2+}}][\mathrm{R{-}OH}] \tag{1.56}$$

Table 1.12: Empirical kinetic adsorption models

Model	Description	Equation	Description of equation
Boyd	Boyd et al. (1947) obtained an expression for Equation 1.45 to calculate the fractional attainment of adsorption equilibrium F as a function of time.	$$F = 1 - \frac{6}{\pi^2}\sum_{n=1}^{\infty}\frac{1}{n^2}\exp\left(-n^2 Bt\right) \quad (1.57)$$	$F = \frac{q}{q_e}$ and $B = \frac{\pi^2 D_e}{r^2}$.
Reichenberg	A piecewise approximation for solving Equation 1.57 derived by Reichenberg (1953) for long and short times.	$$Bt = \begin{cases} 2\pi - \frac{\pi^2 F}{3} - 2\pi\sqrt{1-\frac{\pi F}{3}} & F \leq 0.85 \\ -0.4977 - \ln(1-F) & F > 0.85 \end{cases} \quad (1.58)$$	With F being determined by experimental procedure, Equation 1.58 can be used to solve for Bt and plotted as a function of t. If internal mass transfer is the limiting rate, then the plot should be linear with segments of slope B that can be used to solve for effective diffusivity (El-Khaiary and Malash, 2011).
Weber and Morris	Internal diffusion is frequently analysed in literature using the Weber and Morris model.	$$q = k_{WM} t^{1/2} + c \quad (1.59)$$ $$k_{WM} = 6\frac{q_e}{r}\sqrt{\frac{D_e}{\pi}} \quad (1.60)$$	k_{WM} is the diffusion rate constant and c is a constant (Largitte and Pasquier, 2016). If q is plotted as a function of the square root of time and a single straight line is produced with c = 0, then intraparticle diffusion is the limiting factor. If the plot is multi-linear, then multiple rate limiting steps are involved (Fierro et al., 2008). The slopes of each segment in the plot correspond to k_{WM} and can be used to solve for D_e in Equation 1.60 (Tsibranska and Hristova, 2011).
Langmuir	The integration of Equation 1.51 given by Largitte and Pasquier (2016).	$$q(t) = q_e\frac{k'_a}{k'_a + k_d}\left[1 - e^{-(k'_a + k_d)t}\right] \quad (1.61)$$	k'_a is a pseudo-rate constant representing $k_a C$.

Table 1.12: Empirical kinetic adsorption models

Model	Description	Equation		Description of equation
Pseudo-first-order	Lagergren (1898) derived a model following Langmuir adsorption assumptions (Largitte and Pasquier, 2016; Ho and McKay, 2000) but with the assumption of negligible desorption.	$q\,(t) = q_e\left(1 - e^{-k_1 t}\right)$	(1.62)	k_1 is the pseudo-first-order rate constant (min^{-1}). Kinetics of sites with different binding energies can be represented by fitting adsorption as the sum of multiple pseudo-first-order compartments (Cornelissen et al., 1997)
Pseudo-second-order	The pseudo-second-order model was first developed by Ho and McKay (2000) to describe kinetics of divalent metal adsorption onto sites in competition with hydrogen ions: $2\,\mathrm{S}^- + \mathrm{M}^{2+} \longleftrightarrow \mathrm{MS}_2$ $2\,\mathrm{HS} + \mathrm{M}^{2+} \longleftrightarrow \mathrm{MS}_2 + 2\,\mathrm{H}^+$	$q\,(t) = \dfrac{q_e^2 k_2 t}{1 + q_e k_2 t}$	(1.63)	k_2 is the pseudo-second-order rate constant ($\mathrm{g\,mg^{-1}\,min^{-1}}$).
Elovich	The Elovich kinetic model is a thermodynamic derivation for molecular exchange adsorption which occurs on a heterogeneous surface with activation energy that increases as molecules are adsorbed (Wu et al., 2009; Wang and Guo, 2020).	$q(t) = \dfrac{1}{b}\ln\left(1 + abt\right)$	(1.64)	a is the initial rate of chemisorption ($\mathrm{mg\,g^{-1}\,min^{-1}}$). The significance of b ($\mathrm{g\,mg^{-1}}$) has a variety of descriptions among authors, including representing the deceleration of adsorption (McLintock, 1970), the desorption constant (Tran et al., 2017), and an indication of the number of sites available (Fierro et al., 2008).

Model comparison

Several mathematical tools have been developed for the comparison of models fit to experimental data to determine which model most accurately describes reality.

Coefficient of determination In many studies, the coefficient of determination R^2 is used for model comparison. It is calculated as (El-Khaiary and Malash, 2011):

$$R^2 = 1 - \frac{SS_E}{SS_T} \tag{1.65}$$

Where SS_E is the residual sum of squares and SS_T is the total sum of squares. For a model fit to data points q with predicted values q_{mod}, SS_E and SS_T are given in Equation 1.66 and Equation 1.67 respectively.

$$SS_E = \sum_i \left(q_i - q_{\text{mod},i}\right)^2 \tag{1.66}$$

$$SS_T = \sum_i \left(q_i - \bar{q}\right)^2 \tag{1.67}$$

Here $\bar{q}$ denotes the mean value of q. While R^2 helps determine the accuracy of fit for a model, it is widely discouraged to compare models using it (El-Khaiary and Malash, 2011; Motulsky and Christopoulos, 2003; Montgomery, 2013). This is because R^2 is sensitive to outliers, tends to increase with increases in the range of the independent variable, and it favours models with more parameters (El-Khaiary and Malash, 2011).

Akaike information criterion This criterion, abbreviated as AIC was developed with the purpose of comparing models to determine which one would have the highest likelihood of being accurate (Akaike, 1974). The criterion has been modified into the corrected AIC, or AIC_C, to remove bias found in small sample sizes for non-linear regression (Hurvich and Tsai, 1989). The AIC_C is expressed as (Bolster and Hornberger, 2007):

$$\text{AIC}_\text{C} = n \ln\left(\frac{SS_E}{n}\right) + 2\left(n_p + 1\right) + \frac{2\left(n_p + 1\right)\left(n_p + 2\right)}{n - n_p - 2} \tag{1.68}$$

Where n is the number of data points and n_p is the number of parameters. AIC_C is not unitless, and therefore the criterion only gains meaning when compared

to another criterion of the same units. When considering two models, the probability P that the second model is more accurate than the first is calculated using Equation 1.69 and Equation 1.70 (Motulsky and Christopoulos, 2003):

$$\Delta = \mathrm{AIC}_{\mathrm{C},\,2} - \mathrm{AIC}_{\mathrm{C},\,1} \tag{1.69}$$

$$P = \frac{e^{-0.5\Delta}}{1 + e^{-0.5\Delta}} \tag{1.70}$$

Chapter 2

Experimental

2.1 General experimental procedures

2.1.1 Biosorption material preparation

Cultures were prepared in sterile batch reactors using the B consortium. The 100 mL growth suspension contained 20 g L^{-1} tryptone, 10 g L^{-1} yeast extract, and 1.0 g L^{-1} NaCl (Hörstmann et al., 2020). Culture preparation was done in the absence of lead, but 0.43 g L^{-1} $NaNO_3$ was added to ensure that bacteria were still provided with nitrates previously supplied from $Pb(NO_3)_2$ in experiments done by Hörstmann et al. (2020). Batch reactors were purged with nitrogen for 3 min to ensure anaerobic conditions (Peens, Wu, et al., 2018b) and left to grow in a shaker-incubator for 24 h, 35 °C and 120 rpm. To successfully inhibit the microbial respiratory chain and ensure Pb(II) removal through biosorption alone, the culture was exposed to 50 mM of NaN_3 (Cabrol et al., 2017) for 3 h.

2.1.2 Dry mass measurement

Following the 24 h culture growth period described in Section 2.1.1, a portion of the living bacteria was centrifuged at 9000 rpm for 10 min before being oven dried overnight at 85 °C for weighing.

2.1.3 Plate count

Plate count growth medium was prepared in sterile conditions and consisted of 15 g L^{-1} agar, 20 g L^{-1} tryptone, 10 g L^{-1} yeast extract, and 1.0 g L^{-1} NaCl. Following the 24 h culture growth period described in Section 2.1.1, a portion of

the living bacteria was serially diluted in ultrapure water to the desired concentration. 0.1 mL of diluted solution was thereafter spread onto solid agar plates and incubated at 35 °C for 48 h.

2.1.4 Pb(II) concentration measurement

Samples to be used for Pb(II) removal were diluted with ultrapure water to concentrations between 0 g L^{-1} and 10 g L^{-1}. Analysis was thereafter done with an atomic absorption spectrometer (Perkin Elmer AAnalyst 400, Waltham, Massachusetts).

2.1.5 Metabolic activity measurement

Metabolic activity was measured with 3-(4,5-dimethylthiazol-2-yl)-2,5-diphenyl tetrazolium bromide (MTT). MTT is a yellow dye which is reduced to formazan crystals by the dehydrogenase system of viable gram-negative bacterial cells. MTT solution was prepared using 5 g L^{-1} MTT in ultrapure water.

For metabolic activity readings, filtered (0.45 µm) and unfiltered samples were diluted 4 times and mixed with MTT to form a 10 % MTT solution. The solution was incubated for an hour, after which formazan crystals were dissolved by dimethyl sulfoxide. A spectrophotometer with light at 550 nm was used to measure light absorbed by solution and infer metabolic activity from the difference between filtered and unfiltered samples (Peens, 2018).

2.2 Effect of initial Pb(II) and biomass concentration on equilibrium Pb(II) concentration

2.2.1 Introduction

This section served to assist in experimental planning by provding insight into expected adsorption capacity and Pb removal. Knowledge of the relationship between these three variables also assists in assessing optimum concentrations and efficiency for biosorption by the consortia.

2.2.2 Materials and methods

Dead bacteria culture was prepared as described in Section 2.1.1 and thereafter dispensed in volumes ranging from 0.2 mL to 3.4 mL into serum bottles containing 50 mg L^{-1} to 450 mg L^{-1} Pb(II). To retain the same ionic strength as growth culture, 0.17 M $NaNO_3$ was added into serum bottles.

Serum bottles were left for 3 h before samples were taken from each reactor and filtered. Pb(II) concentration and metabolic activity were measured at the beginning and at equilibrium.

2.2.3 Results and discussion

Metabolic activity was undetected at the experiment initialisation and equilibrium, indicating successful inhibition of microbial activity by NaN_3.

Figure 2.1 (a) shows a clear increase in Pb(II) removal with higher biomass concentrations. This effect becomes less pronounced as biomass increases, and suggests that increments beyond 47.5 mg L^{-1} may lead to insignificant increases in lead removal. The decrease in adsorption efficiency with an increase in biomass is likely caused by a screen effect, where higher cell densities result in the blocking of active sites (Hammaini et al., 2007). The range studied also shows peak lead removal at initial concentrations around 130 mg L^{-1} lead, regardless of how much biomass is present.

Figure 2.1 (b) illustrates how adsorption capacities of all biosorption concentrations fall on the same isotherm with a $q_{\max}$ of around 2700 mg g^{-1}. The cluster of low adsorption capacities at $C_e > 200$ mg g^{-1} is likely caused by errors introduced by dilutions, as a decrease in adsorption capacity with as C_e increases does not fit a known isotherm type (Alothman, 2012).

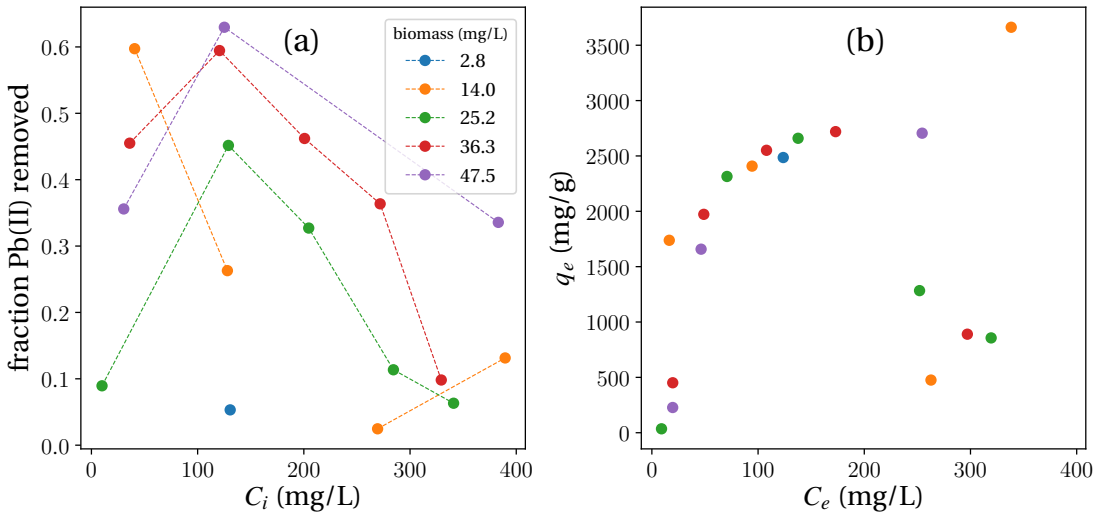

Figure 2.1: The effects of biomass concentration and initial Pb(II) concentration on Pb(II) removal (a) and adsorption capacity (b). The legend shows dry biomass concentration and is shared between both plots.

2.3 Titration

2.3.1 Introduction

2.3.2 Materials and methods

Acid-base titrations of prepared cultures were performed using an autotitrator (Metrohm 848 Titrino Plus).

Standard solutions of 0.1 M HNO_3 and 0.1 M NaOH were used.

Cells prepared dynamic equivalence point titration with autotitrator (Metrohm 848 Titrino Plus). stability of 50.0 mV/min

100 mL samples purged for 5 min with N2 and maintained throughout experiment. temp control at 37 +- 1 Celsius 0.1 M NaOH and HNO3 acid added until a pH of 4 reached, increased with NaOH until 10. pH range outside causes cell damage (less than 3) and lysis (greater than 10) (()Kapetas2011).

2.3.3 Results and discussion

2.4 Adsorption kinetics

2.5 Adsorption equilibrium

References

Akaike, H (1974). "A New Look at the Statistical Model Identification". In: *IEEE Transactions on Automatic Control* 19.6, pp. 716–723. ISSN: 15582523. DOI: 10.1109/TAC.1974.1100705.

Alothman, ZA (2012). "A review: Fundamental aspects of silicate mesoporous materials". In: *Materials* 5.12, pp. 2874–2902. ISSN: 19961944. DOI: 10.3390/ma5122874.

Anastopoulos, I and GZ Kyzas (2015). "Progress in batch biosorption of heavy metals onto algae". In: *Journal of Molecular Liquids* 209, pp. 77–86. ISSN: 01677322. DOI: 10.1016/j.molliq.2015.05.023. URL: http://dx.doi.org/10.1016/j.molliq.2015.05.023.

Ayangbenro, AS and OO Babalola (2017). "A new strategy for heavy metal polluted environments: A review of microbial biosorbents". In: *International Journal of Environmental Research and Public Health* 14.1. ISSN: 16604601. DOI: 10.3390/ijerph14010094.

Ayawei, N, AN Ebelegi, and D Wankasi (2017). *Modelling and Interpretation of Adsorption Isotherms*. DOI: 10.1155/2017/3039817.

Azizian, S (2004). "Kinetic models of sorption: A theoretical analysis". In: *Journal of Colloid and Interface Science* 276.1, pp. 47–52. ISSN: 00219797. DOI: 10.1016/j.jcis.2004.03.048.

Bolster, CH and GM Hornberger (2007). "On the Use of Linearized Langmuir Equations". In: *Soil Science Society of America Journal* 71.6, pp. 1796–1806. ISSN: 0361-5995. DOI: 10.2136/sssaj2006.0304.

Boyd, GE, AW Adamson, and LS Myers (1947). "The Exchange Adsorption of Ions from Aqueous Solutions by Organic Zeolites. II. Kinetics". In: *Journal of the American Chemical Society* 69.11, pp. 2836–2848. ISSN: 15205126. DOI: 10.1021/ja01203a066.

Brink, HG, C Hörstmann, and C Feucht (2019). "Microbial Pb(II) Precipitation: Minimum Inhibitory Concentration and Precipitate Identity". In: *Chemical Engineering Transactions* 74.2019, pp. 1453–1458.

Brink, HG, M Lategan, K Naudé, and EMN Chirwa (2017). "Lead removal using industrially sourced consortia: Influence of lead and glucose concentra-

tions". In: *Chemical Engineering Transactions* 57, pp. 409–414. ISSN: 22839216. DOI: 10.3303/CET1757069.

Brink, HG and Z Mahlangu (2018). "Microbial Lead(II) Precipitation: the Influence of Growth Substrate". In: *Chemical Engineering Transactions* 64.May, pp. 439–444. ISSN: 22839216. DOI: 10.3303/CET1864074.

Brouers, F and TJ Al-Musawi (2015). "On the optimal use of isotherm models for the characterization of biosorption of lead onto algae". In: *Journal of Molecular Liquids* 212, pp. 46–51. ISSN: 01677322. DOI: 10.1016/j.molliq.2015.08.054. URL: http://dx.doi.org/10.1016/j.molliq.2015.08.054.

Cabrol, L, M Quéméneur, and B Misson (2017). "Inhibitory effects of sodium azide on microbial growth in experimental resuspension of marine sediment". In: *Journal of Microbiological Methods* 133, pp. 62–65. ISSN: 18728359. DOI: 10.1016/j.mimet.2016.12.021. URL: http://dx.doi.org/10.1016/j.mimet.2016.12.021.

Chakraborty, S, A Mukherjee, and TP Das (2013). "Biochemical characterization of a lead-tolerant strain of Aspergillus foetidus: An implication of bioremediation of lead from liquid media". In: *International Biodeterioration & Biodegradation* 84, pp. 134–142.

Chan, LS, WH Cheung, SJ Allen, and G McKay (2012). "Error analysis of adsorption isotherm models for acid dyes onto bamboo derived activated carbon". In: *Chinese Journal of Chemical Engineering* 20.3, pp. 535–542. ISSN: 10049541. DOI: 10.1016/S1004-9541(11)60216-4. URL: http://dx.doi.org/10.1016/S1004-9541(11)60216-4.

Chang, E, AW Brewer, DM Park, Y Jiao, and LN Lammers (2020). "Surface complexation model of rare earth element adsorption onto bacterial surfaces with lanthanide binding tags". In: *Applied Geochemistry* 112.November 2019, p. 104478. ISSN: 18729134. DOI: 10.1016/j.apgeochem.2019.104478. URL: https://doi.org/10.1016/j.apgeochem.2019.104478.

Chang, JS, R Law, and CC Chang (1997). "Biosorption of lead, copper and cadmium by biomass of Pseudomonas aeruginosa PU21". In: *Water Research* 31.7, pp. 1651–1658. ISSN: 00431354. DOI: 10.1016/S0043-1354(97)00008-0.

Chatterjee, S, A Mukherjee, A Sarkar, and P R. (2012). "Bioremediation of lead by lead-resistant microorganisms, isolated from industrial sample". In: *Advances in Bioscience and Biotechnology* 03.03, pp. 290–295.

Chen, G, Y Liu, F Liu, and X Zhang (2014). "Fabrication of three-dimensional graphene foam with high electrical conductivity and large adsorption capability". In: *Applied Surface Science* 311, pp. 808–815. ISSN: 01694332. DOI: 10.1016/j.apsusc.2014.05.171. URL: http://dx.doi.org/10.1016/j.apsusc.2014.05.171.

Chen, JP and L Yang (2006). "Study of a heavy metal biosorption onto raw and chemically modified Sargassum sp. via spectroscopic and modeling analysis". In: *Langmuir* 22.21, pp. 8906–8914. ISSN: 07437463. DOI: 10.1021/la060770+.

Chimhundi, J, HG Brink, and EMN Chirwa (2020). "Microbial Removal of Pb(II) by a Continuous Upflow Anaerobic Sludge-Blanket Reactor (CUASBR)". In: *South African Chemical Engineering Congress*.

Choi, SB and YS Yun (2004). "Lead biosorption by waste biomass of Corynebacterium glutamicum generated from lysine fermentation process". In: *Biotechnology Letters* 26.4, pp. 331–336. ISSN: 01415492. DOI: 10.1023/B:BILE.0000015453.20708.fc.

Cornelissen, G, PC Van Noort, JR Parsons, and HA Govers (1997). "Temperature dependence of slow adsorption and desorption kinetics of organic compounds in sediments". In: *Environmental Science and Technology* 31.2, pp. 454–460. ISSN: 0013936X. DOI: 10.1021/es960300+.

Costa, JFSS, VJ Vilar, CM Botelho, EA da Silva, and RA Boaventura (2010). "Application of the Nernst-Planck approach to lead ion exchange in Ca-loaded Pelvetia canaliculata". In: *Water Research* 44.13, pp. 3946–3958. ISSN: 00431354. DOI: 10.1016/j.watres.2010.04.033.

Dada, AO, AP Olalekan, AM Olatunya, and O Dada (2012). "Langmuir, Freundlich, Temkin and DubininRadushkevich Isotherms Studies of Equilibrium Sorption of Zn 2+ Unto Phosphoric Acid Modified Rice Husk". In: *IOSR Journal of Applied Chemistry* 3.1, pp. 38–45. DOI: 10.9790/5736-0313845.

Dai, X, MI Jeffrey, and PL Breuer (2010). "A mechanistic model of the equilibrium adsorption of copper cyanide species onto activated carbon". In: *Hydrometallurgy* 101.3-4, pp. 99–107. ISSN: 0304386X. DOI: 10.1016/j.hydromet.2009.12.005. URL: http://dx.doi.org/10.1016/j.hydromet.2009.12.005.

De, J, N Ramaiah, and L Vardanyan (2008). "Detoxification of Toxic Heavy Metals by Marine Bacteria Highly Resistant to Mercury". In: *Mar Biotechnol* 10, pp. 471–477.

Department of Water Affairs and Forestry (1998). *Minimum requirements for the handling, classification and disposal of hazardous waste*. Ed. by K Langmore. Second Edi. ISBN: 0620229950.

Duncan, JR, A Stoll, B Wilhelmi, M Zhao, and R van Hille (2003). *The use of algal and yeast biomass to accumulate toxic and valuable heavy metals from wastewater: WEC Report No. 616/1/03*. Tech. rep. Water Research Comission.

Edzwald, J (2011). *Water Quality & Treatment: A Handbook on Drinking Water*. Sixth Edit. McGraw-Hill Professional. ISBN: 0070016593. DOI: 10.1002/047147844X.pc1506.

Esposito, A, F Pagnanelli, and F Vegliò (2002). "pH-related equilibria models for biosorption in single metal systems". In: *Chemical Engineering Science* 57.3, pp. 307–313. ISSN: 00092509. DOI: 10.1016/S0009-2509(01)00399-2.

Farhan, SN and AA Khadom (2015). "Biosorption of heavy metals from aqueous solutions by Saccharomyces Cerevisiae". In: *International Journal of Industrial Chemistry* 6.2, pp. 119–130. ISSN: 22285547. DOI: 10.1007/s40090-015-0038-8. URL: http://dx.doi.org/10.1007/s40090-015-0038-8.

Fein, JB, CJ Daughney, N Yee, and TA Davis (1997). "A chemical equilibrium model for metal adsorption onto bacterial surfaces". In: *Geochimica et Cosmochimica Acta* 61.16, pp. 3319–3328. ISSN: 00167037. DOI: 10.1016/S0016-7037(97)00166-X.

Fierro, V, V Torné-Fernández, D Montané, and A Celzard (2008). "Adsorption of phenol onto activated carbons having different textural and surface properties". In: *Microporous and Mesoporous Materials* 111.1-3, pp. 276–284. ISSN: 13871811. DOI: 10.1016/j.micromeso.2007.08.002.

Fogler, HS (2006). *Elements of Chemical Reaction Engineering, Fourth Edition*. Prentice Hall Professional Technical Reference, pp. 661–665. ISBN: 9781292026169.

Fomina, M and GM Gadd (2014). "Biosorption: Current perspectives on concept, definition and application". In: *Bioresource Technology* 160, pp. 3–14. ISSN: 18732976. DOI: 10.1016/j.biortech.2013.12.102. URL: http://dx.doi.org/10.1016/j.biortech.2013.12.102.

Foo, KY and BH Hameed (2010). "Insights into the modeling of adsorption isotherm systems". In: *Chemical Engineering Journal* 156.1, pp. 2–10. ISSN: 13858947. DOI: 10.1016/j.cej.2009.09.013.

Fu, F and Q Wang (2011). "Removal of heavy metal ions from wastewaters: A review". In: *Journal of Environmental Management* 92.3, pp. 407–418.

Gadd, GM and J Griffiths (1977). "Microorganisms and heavy metal toxicity". In: *Microbial Ecology* 4.4, pp. 303–317. ISSN: 1432184X. DOI: 10.1007/BF02013274.

Goldberg, S (1995). "Adsorption Models Incorporated into Chemical Equilibrium Models". In: *Chemical Equilibrium and Reaction Models*. Soil Science Society of America. Chap. 5, pp. 75–95. DOI: 10.1201/9780203734117-5.

Grivé, M, C Domènech, V Montoya, D García, and L Duro (2010). *Determination and assessment of the concentration limits to be used in SR-Can, Supplement to TR-06-32*. Tech. rep. January. Swedish Nuclear Fuel and Waste Management Co, p. 32.

Guiza, S (2017). "Biosorption of heavy metal from aqueous solution using cellulosic waste orange peel". In: *Ecological Engineering*. ISSN: 09258574. DOI: 10.1016/j.ecoleng.2016.11.043.

Haas, JR, TJ Dichristina, and R Wade (2001). "Thermodynamics of U(VI) sorption onto Shewanella putrefaciens". In: *Chemical Geology* 180.1-4, pp. 33–54. ISSN: 00092541. DOI: 10.1016/S0009-2541(01)00304-7.

Hammaini, A, F González, A Ballester, ML Blázquez, and JA Muñoz (2007). "Biosorption of heavy metals by activated sludge and their desorption characteristics". In: *Journal of Environmental Management* 84.4, pp. 419–426. ISSN: 03014797. DOI: 10.1016/j.jenvman.2006.06.015.

Ho, YS and G McKay (2000). "The kinetics of sorption of divalent metal ions onto sphagnum moss peat". In: *Water Research* 34.3, pp. 735–742. ISSN: 00431354. DOI: 10.1016/S0043-1354(99)00232-8.

Hörstmann, C (2019). "Factors affecting viability of, and Pb(II)-removal by, Pb (II) resistant microbial consortia." PhD thesis. University of Pretoria.

Hörstmann, C, HG Brink, and EM Chirwa (2020). "Pb(II) Bio-Removal, Viability, and Population Distribution of an Industrial Microbial Consortium: The Effect of Pb(II) and Nutrient Concentrations". In: *Sustainabilty* March. DOI: 10.3390/su12062511.

Hu, X, J Cao, H Yang, D Li, Y Qiao, J Zhao, Z Zhang, and L Huang (2020). "Pb2+ biosorption from aqueous solutions by live and dead biosorbents of the hydrocarbon-degrading strain Rhodococcus sp. HX-2". In: *PLoS ONE* 15.1. ISSN: 19326203. DOI: 10.1371/journal.pone.0226557.

Huang, CP and J Wang (2014). "Specific chemical interactions between metal ions and biological solids exemplified by sludge particulates". In: *Bioresource Technology* 160, pp. 32–42. ISSN: 18732976. DOI: 10.1016/j.biortech.2014.01.043. URL: http://dx.doi.org/10.1016/j.biortech.2014.01.043.

Huang, W and ZM Liu (2013). "Biosorption of Cd(II)/Pb(II) from aqueous solution by biosurfactant-producing bacteria: Isotherm kinetic characteristic and mechanism studies". In: *Colloids and Surfaces B: Biointerfaces* 105, pp. 113–119. ISSN: 09277765. DOI: 10.1016/j.colsurfb.2012.12.040. URL: http://dx.doi.org/10.1016/j.colsurfb.2012.12.040.

Hurvich, CM and CL Tsai (1989). "Regression and time series model selection in small samples". In: *Biometrika* 76.2, pp. 297–307. ISSN: 00063444. DOI: 10.1093/biomet/76.2.297.

ILA (2019). *Lead Production & Statistics*. URL: https://www.ila-lead.org/lead-facts/lead-production-statistics.

Inyinbor, AA, FA Adekola, and GA Olatunji (2016). "Kinetics, isotherms and thermodynamic modeling of liquid phase adsorption of Rhodamine B dye onto Raphia hookerie fruit epicarp". In: *Water Resources and Industry* 15, pp. 14–27. ISSN: 22123717. DOI: 10.1016/j.wri.2016.06.001. URL: http://dx.doi.org/10.1016/j.wri.2016.06.001.

Jeppu, GP and TP Clement (2012). "A modified Langmuir-Freundlich isotherm model for simulating pH-dependent adsorption effects". In: *Journal of Contaminant Hydrology* 129-130, pp. 46–53. ISSN: 01697722. DOI: 10.1016/j.jconhyd.2011.12.001. URL: http://dx.doi.org/10.1016/j.jconhyd.2011.12.001.

Kang, CH, SJ Oh, YJ Shin, SH Han, IH Nam, and JS So (2015). "Bioremediation of lead by ureolytic bacteria isolated from soil at abandoned metal mines in South Korea". In: *Ecological Engineering* 74, pp. 402–407. ISSN: 09258574. DOI: 10.1016/j.ecoleng.2014.10.009. URL: http://dx.doi.org/10.1016/j.ecoleng.2014.10.009.

El-Khaiary, MI and GF Malash (2011). "Common data analysis errors in batch adsorption studies". In: *Hydrometallurgy* 105.3-4, pp. 314–320. ISSN: 0304386X. DOI: 10.1016/j.hydromet.2010.11.005. URL: http://dx.doi.org/10.1016/j.hydromet.2010.11.005.

Knops, M, R Altenburger, and H Segner (2001). "Alterations of physiological energetics, growth and reproduction of Daphnia magna under toxicant stress". In: *Aquatic Toxicology* 53.2, pp. 79–90. ISSN: 0166445X. DOI: 10.1016/S0166-445X(00)00170-3.

Kotz, JC, PM Treichel, J Townsend, and D Treichel (2014). *Chemistry & Chemical Reactivity*. 9th ed. Cengage Learning. ISBN: 9781133949640.

Kumar Reddy, DH and S Lee (2012). "Water Pollution and Treatment Technologies". In: *Journal of Environmental & Analytical Toxicology* 02.05. DOI: 10.4172/2161-0525.1000e103.

Kushwaha, A, R Rani, S Kumar, T Thomas, AA David, and M Ahmed (2017). "A new insight to adsorption and accumulation of high lead concentration by exopolymer and whole cells of lead-resistant bacterium Acinetobacter junii L. Pb1 isolated from coal mine dump". In: *Environmental Science and Pollution Research* 24.11, pp. 10652–10661. ISSN: 16147499. DOI: 10.1007/s11356-017-8752-8.

Lagergren, SY (1898). "Zur Theorie der sogenannten Adsorption gelöster Stoffe". In: *Kungliga Svenska Vetenskapsakademiens* 24.4, pp. 1–39.

Langmuir, I (1918). "The adsorption of gases on plane surfaces of glass, mica and platinum". In: *Journal of the American Chemical Society* 40.9, pp. 1361–1403. ISSN: 15205126. DOI: 10.1021/ja02242a004.

Largitte, L and R Pasquier (2016). "A review of the kinetics adsorption models and their application to the adsorption of lead by an activated carbon". In: *Chemical Engineering Research and Design* 109, pp. 495–504. ISSN: 02638762. DOI: 10.1016/j.cherd.2016.02.006. URL: http://dx.doi.org/10.1016/j.cherd.2016.02.006.

Lawrence, RW, RMR Branion, and HG Ebner (1985). "Fundamental and applied biohydrometallurgy". In: *Proceedings of the Sixth International Symposium on Biohydrometallurgy, Vancouver, B.C., Canada, August 21-24, 1985*. Elsevier, pp. 279–289.

Lee, SH, JS Shon, H Chung, MY Lee, and JW Yang (1999). "Effect of Chemical Modification of Carboxyl Groups in Apple Residues on Metal Ion Binding". In: *Korean Journal of Chemical Engineering* 16.5, pp. 576–580. ISSN: 02561115. DOI: 10.1007/BF02708134.

Levinson, H, I Mahler, P Blackwelder, and T Hood (1996). "Lead resistance and sensitivity in Staphylococcus aureus ". In: *FEMS Microbiology Letters* 145, pp. 421–425.

Li, H, X Dong, EB da Silva, LM de Oliveira, Y Chen, and LQ Ma (2017). "Mechanisms of metal sorption by biochars: Biochar characteristics and modifications". In: *Chemosphere* 178, pp. 466–478. ISSN: 18791298. DOI: 10.1016/j.chemosphere.2017.03.072. URL: http://dx.doi.org/10.1016/j.chemosphere.2017.03.072.

Lin, CC and YT Lai (2006). "Adsorption and recovery of lead(II) from aqueous solutions by immobilized Pseudomonas Aeruginosa PU21 beads". In: *Journal of Hazardous Materials* 137.1, pp. 99–105. ISSN: 03043894. DOI: 10.1016/j.jhazmat.2006.02.071.

Liu, H and HH Fang (2002). "Extraction of extracellular polymeric substances (EPS) of sludges". In: *Journal of Biotechnology* 95.3, pp. 249–256. ISSN: 01681656. DOI: 10.1016/S0168-1656(02)00025-1.

Lu, H, W Zhang, Y Yang, X Huang, S Wang, and R Qiu (2012). "Relative distribution of Pb 2+ sorption mechanisms by sludge-derived biochar". In: *Water Research* 46.3, pp. 854–862. ISSN: 00431354. DOI: 10.1016/j.watres.2011.11.058. URL: http://dx.doi.org/10.1016/j.watres.2011.11.058.

Lu, WB, JJ Shi, CH Wang, and JS Chang (2006). "Biosorption of lead, copper and cadmium by an indigenous isolate Enterobacter sp. J1 possessing high heainitialsvy-metal resistance". In: *Journal of Hazardous Materials* 134.1-3, pp. 80–86. ISSN: 03043894. DOI: 10.1016/j.jhazmat.2005.10.036.

Lützenkirchen, J (1999). "Parameter estimation for the constant capacitance surface complexation model: Analysis of parameter interdependencies". In: *Journal of Colloid and Interface Science* 210.2, pp. 384–390. ISSN: 00219797. DOI: 10.1006/jcis.1998.5956.

Mader, SS (1998). *Biology, Sixth Edition*. WCB McGraw-Hill. ISBN: 9780075617334.

Masoumi, F, E Khadivinia, L Alidoust, Z Mansourinejad, S Shahryari, M Safaei, A Mousavi, AH Salmanian, HS Zahiri, H Vali, and KA Noghabi (2016). "Nickel and lead biosorption by Curtobacterium sp. FM01, an indigenous bacterium isolated from farmland soils of northeast Iran". In: *Journal of Environmen-*

tal Chemical Engineering 4.1, pp. 950–957. ISSN: 22133437. DOI: 10.1016/j.jece.2015.12.025. URL: http://dx.doi.org/10.1016/j.jece.2015.12.025.

Mathew, BB and NB Krishnamurthy (2018). "Screening and identification of bacteria isolated from industrial area groundwater to study lead sorption: Kinetics and statistical optimization of biosorption parameters". In: *Groundwater for Sustainable Development* 7.August, pp. 313–327. ISSN: 2352801X. DOI: 10.1016/j.gsd.2018.07.007. URL: https://doi.org/10.1016/j.gsd.2018.07.007.

McLintock, IS (1970). "Comments on the Elovich equation". In: *Journal of Catalysis* 16.1, pp. 126–128. ISSN: 10902694. DOI: 10.1016/0021-9517(70)90204-6.

Montgomery, DC (2013). *Design and Analysis of Experiments (8th Edition)*. John Wiley & Sons. ISBN: 978-1-118-14692-7.

Motulsky, H and A Christopoulos (2003). *Fitting models to biological data using linear and nonlinear regression. A practical guide to curve fitting*. GraphPad Software Inc. ISBN: 9780195171808. DOI: 10.1002/pst.167.

Mudipalli, A (2007). "Lead hepatotoxicity & potential health effects". In: *Indian Journal of Medical Research* 126.6, pp. 518–527.

Naik, MM and SK Dubey (2013). "Lead resistant bacteria: Lead resistance mechanisms, their applications in lead bioremediation and biomonitoring". In: *Ecotoxicology and Environmental Safety* 98, pp. 1–7. ISSN: 01476513. DOI: 10.1016/j.ecoenv.2013.09.039. URL: http://dx.doi.org/10.1016/j.ecoenv.2013.09.039.

National Center for Biotechnology Information (2020a). *LPS with O-antigen, CID=53481793*. URL: https://pubchem.ncbi.nlm.nih.gov/compound/LPS-with-O-antigen (visited on 05/01/2020).

National Center for Biotechnology Information (2020b). *Peptidoglycan(N-acetyl-D-glucosamine), CID=5462260*. URL: https://pubchem.ncbi.nlm.nih.gov/compound/Peptidoglycan%7B%5C_%7DN-acetyl-D-glucosamine (visited on 05/01/2020).

Ngwenya, BT, JFW Mosselmans, M Magennis, KD Atkinson, J Tourney, V Olive, and RM Ellam (2009). "Macroscopic and spectroscopic analysis of lanthanide adsorption to bacterial cells". In: *Geochimica et Cosmochimica Acta* 73.11, pp. 3134–3147. ISSN: 00167037. DOI: 10.1016/j.gca.2009.03.018. URL: http://dx.doi.org/10.1016/j.gca.2009.03.018.

Ngwenya, BT, IW Sutherland, and L Kennedy (2003). "Comparison of the acid-base behaviour and metal adsorption characteristics of a gram-negative bacterium with other strains". In: *Applied Geochemistry* 18.4, pp. 527–538. ISSN: 08832927. DOI: 10.1016/S0883-2927(02)00118-X.

Ngwenya, N and EM Chirwa (2015). "Characterisation of surface uptake and biosorption of cationic nuclear fission products by sulphate-reducing bacteria". In: *Water SA* 41.3, pp. 314–324. ISSN: 18167950. DOI: 10.4314/wsa.v41i3.03.

Ohshima, H and T Kondo (1990). "Relationship among the surface potential, Donnan potential and charge density of ion-penetrable membranes". In: *Biophysical Chemistry* 38.1-2, pp. 117–122. ISSN: 03014622. DOI: 10.1016/0301-4622(90)80046-A.

Okoro, HK, OS Fatoki, Fa Adekola, BJ Ximba, RG Snyman, and B Opeolu (2011). "Oil Palm biomass as an adsorbent for heavy metals". In: *Reviews of Environmental Contamination and Toxicology* 232.April, pp. 61–88. ISSN: 01795953. DOI: 10.1007/978-1-4419-9860-6. URL: http://link.springer.com/10.1007/978-1-4419-8011-3%7B%5C%%7D5Cnhttp://www.springerlink.com/index/10.1007/978-1-4419-9860-6.

Pagnanelli, F, S Mainelli, and L Toro (2005). "Optimisation and validation of mechanistic models for heavy metal bio-sorption onto a natural biomass". In: *Hydrometallurgy* 80.1-2, pp. 107–125. ISSN: 0304386X. DOI: 10.1016/j.hydromet.2005.07.008.

Patra, RC, AK Rautray, and D Swarup (2011). "Oxidative stress in lead and cadmium toxicity and its amelioration". In: *Veterinary Medicine International* 2011. ISSN: 20420048. DOI: 10.4061/2011/457327.

Peens, J, WY Wu, and HG Brink (2018a). "Microbial Pb(II) Precipitation: The Influence of Elevated Pb(II) Concentrations". In: *Chemical Engineering Transactions* 64.2018, pp. 439–444.

Peens, J (2018). "Pb (II)-Removal From Water Using Microorganisms Naturally Evolved to Tolerate Pb(II) -Toxicity Pb (II) -Removal From Water Using Microorganisms Naturally Evolved to Tolerate Pb (II)-Toxicity". PhD thesis. University of Pretoria.

Peens, J, YW Wu, and HG Brink (2018b). "Microbial Pb(II) precipitation: The influence of elevated Pb(II) Concentrations". In: *Chemical Engineering Transactions* 64.ii, pp. 583–588. ISSN: 22839216. DOI: 10.3303/CET1864098.

Philp, JC, SM Barnforth, I Singleton, and RM Atlas (2005). "Environmental Pollution and Restoration: A Role for Bioremediation". In: *Bioremediation Applied Microbial Solutions for Real-World Environmental Cleanup*. Washington, D.C.: ASM Press, pp. 1–24.

Puyen, ZM, E Villagrasa, J Maldonado, E Diestra, I Esteve, and A Solé (2012). "Biosorption of lead and copper by heavy-metal tolerant Micrococcus luteus DE2008". In: *Bioresource Technology* 126, pp. 233–237. ISSN: 18732976. DOI: 10.1016/j.biortech.2012.09.036. URL: http://dx.doi.org/10.1016/j.biortech.2012.09.036.

Qin, H, T Hu, Y Zhai, N Lu, and J Aliyeva (2020). "The improved methods of heavy metals removal by biosorbents: A review". In: *Environmental Pollution* 258, p. 113777. ISSN: 18736424. DOI: 10.1016/j.envpol.2019.113777. URL: https://doi.org/10.1016/j.envpol.2019.113777.

Rangabhashiyam, S and P Balasubramanian (2019). "Characteristics, performances, equilibrium and kinetic modeling aspects of heavy metal removal using algae". In: *Bioresource Technology Reports* 5.August 2018, pp. 261–279. ISSN: 2589014X. DOI: 10.1016/j.biteb.2018.07.009. URL: https://doi.org/10.1016/j.biteb.2018.07.009.

Reichenberg, D (1953). "Properties of Ion-Exchange Resins in Relation to their Structure. III. Kinetics of Exchange". In: *Journal of the American Chemical Society* 75.3, pp. 589–597. ISSN: 15205126. DOI: 10.1021/ja01099a022.

Ren, G, Y Jin, C Zhang, H Gu, and J Qu (2015). "Characteristics of Bacillus sp. PZ-1 and its biosorption to Pb(II)". In: *Ecotoxicology and Environmental Safety* 117, pp. 141–148. ISSN: 10902414. DOI: 10.1016/j.ecoenv.2015.03.033. URL: http://dx.doi.org/10.1016/j.ecoenv.2015.03.033.

Robalds, A, GM Naja, and M Klavins (2016). "Highlighting inconsistencies regarding metal biosorption". In: *Journal of Hazardous Materials* 304, pp. 553–556. ISSN: 18733336. DOI: 10.1016/j.jhazmat.2015.10.042.

Rosenberg, E, EF Delong, and F Thompson (2013). *The Prokaryotes*. Fourth Edi. Springer-Verlag. ISBN: 9783642301933.

Saha, GC, MIU Hoque, MAM Miah, R Holze, DA Chowdhury, S Khandaker, and S Chowdhury (2017). "Biosorptive removal of lead from aqueous solutions onto Taro (Colocasiaesculenta(L.) Schott) as a low cost bioadsorbent: Characterization, equilibria, kinetics and biosorption-mechanism studies". In: *Journal of Environmental Chemical Engineering* 5.3, pp. 2151–2162. ISSN: 22133437. DOI: 10.1016/j.jece.2017.04.013. URL: http://dx.doi.org/10.1016/j.jece.2017.04.013.

Salehizadeh, H and SA Shojaosadati (2003). "Removal of metal ions from aqueous solution by polysaccharide produced from Bacillus firmus". In: *Water Research* 37.17, pp. 4231–4235. ISSN: 00431354. DOI: 10.1016/S0043-1354(03)00418-4.

Selatnia, A, A Boukazoula, N Kechid, MZ Bakhti, A Chergui, and Y Kerchich (2004). "Biosorption of lead (II) from aqueous solution by a bacterial dead Streptomyces rimosus biomass". In: *Biochemical Engineering Journal* 19.2, pp. 127–135. ISSN: 1369703X. DOI: 10.1016/j.bej.2003.12.007.

Seung Kim, Y and C Rae Park (2016). "Titration Method for the Identification of Surface Functional Groups". In: *Materials Science and Engineering of Carbon*, pp. 273–286. DOI: 10.1016/b978-0-12-805256-3.00013-1.

Shakoor, M, S Ali, M Farid, M Farooq, H Tauqeer, U Iftikhar, F Hannan, and S Bharwana (2013). "Heavy metal pollution, a global problem and its remediation by chemically enhanced phytoremediation: A Review". In: *Journal of Biodiversity and Environmental Sciences* 3.3, pp. 12–20.

Smith, JG (2014). *Organic Chemistry*. 4th ed. McGraw-Hill. ISBN: 9789814581882.

Statista (2019). *Lead reserves worldwide by country 2018 (in million metric tons)*. URL: https://www.statista.com/statistics/273652/global-lead-reserves-by-selected-countries/.

Stumm, W (1992). *Chemistry of the SolidWater Interface: Processes at the MineralWater and ParticleWater Interface in Natural Systems*. John Wiley & Sons. ISBN: 9780471576723.

Suzuki, M (1990). *Adsorption Engineering*. Tokyo: Elsevier B.V.

Tran, HN, SJ You, A Hosseini-Bandegharaei, and HP Chao (2017). "Mistakes and inconsistencies regarding adsorption of contaminants from aqueous solutions: A critical review". In: *Water Research* 120, pp. 88–116. ISSN: 18792448. DOI: 10.1016/j.watres.2017.04.014. URL: http://dx.doi.org/10.1016/j.watres.2017.04.014.

Tsibranska, I and E Hristova (2011). "Comparison of different kinetic models for adsorption of heavy metals onto activated carbon from apricot stones". In: *Bulgarian Chemical Communications* 43.3, pp. 370–377. ISSN: 08619808.

Tunali, S, A Çabuk, and T Akar (2006). "Removal of lead and copper ions from aqueous solutions by bacterial strain isolated from soil". In: *Chemical Engineering Journal* 115.3, pp. 203–211. ISSN: 13858947. DOI: 10.1016/j.cej.2005.09.023.

Turner, BF (2005). "ProtoFit Version 2.0 A program for determining surface speciation constants from titration data USER'S MANUAL". In: *Dept. of Civil Engineering and Geological Sciences 156 Fitzpatrick Hall University of Notre Dame Notre Dame, IN 46556*. URL: http://protofit.sourceforge.net/protofit%7B%5C_%7Ddocs.html.

UNEP (2010). *Final Review of Scientific Information on Lead*. UNEP-DTIE Chemicals Branch.

Unuabonah, EI, MO Omorogie, and NA Oladoja (2019). *Modeling in Adsorption: Fundamentals and Applications*, pp. 85–118. ISBN: 9780128141328. DOI: 10.1016/b978-0-12-814132-8.00005-8.

Uslu, G and M Tanyol (2006). "Equilibrium and thermodynamic parameters of single and binary mixture biosorption of lead (II) and copper (II) ions onto Pseudomonas putida: Effect of temperature". In: *Journal of Hazardous Materials* 135.1-3, pp. 87–93. ISSN: 03043894. DOI: 10.1016/j.jhazmat.2005.11.029.

Van Hille, RP, A Antunes, D Sanyahumbi, L Nightingale, and JR Duncan (2003). *Development of integrated biosorption systems for the removal and/or recovery of heavy metals from mining and other industrial wastewaters, and determination of the toxicity of metals to bioremediation processes: WRC Report No. 1243/1/03*. Tech. rep. Water Research Comission.

Veglió, F, F Beolchini, and A Gasbarro (1997). "Biosorption of toxic metals: An equilibrium study using free cells of Arthrobacter sp." In: *Process Biochemistry* 32.2, pp. 99–105. ISSN: 13595113. DOI: 10.1016/S0032-9592(96)00047-7.

Verma, A, S Kumar, and S Kumar (2016). "Biosorption of lead ions from the aqueous solution by Sargassum filipendula: Equilibrium and kinetic studies". In: *Journal of Environmental Chemical Engineering* 4.4, pp. 4587–4599. ISSN: 22133437. DOI: 10.1016/j.jece.2016.10.026. URL: http://dx.doi.org/10.1016/j.jece.2016.10.026.

Vijayaraghavan, K and YS Yun (2008). "Bacterial biosorbents and biosorption". In: *Biotechnology Advances* 26.3, pp. 266–291. ISSN: 07349750. DOI: 10.1016/j.biotechadv.2008.02.002.

Villarreal, MR (2008). *Average prokaryote cell*. URL: https://commons.wikimedia.org/wiki/File:Average%7B%5C_%7Dprokaryote%7B%5C_%7Dcell-%7B%5C_%7Dunlabled.svg.

Volesky, B (2007). "Biosorption and me". In: *Water Research* 41.18, pp. 4017–4029. ISSN: 00431354. DOI: 10.1016/j.watres.2007.05.062.

Wang, J and C Chen (2009). "Biosorbents for heavy metals removal and their future". In: *Biotechnology Advances* 27.2, pp. 195–226. ISSN: 07349750. DOI: 10.1016/j.biotechadv.2008.11.002. URL: http://dx.doi.org/10.1016/j.biotechadv.2008.11.002.

Wang, J and X Guo (2020). "Adsorption kinetic models: Physical meanings, applications, and solving methods". In: *Journal of Hazardous Materials* 390.January, p. 122156. ISSN: 18733336. DOI: 10.1016/j.jhazmat.2020.122156. URL: https://doi.org/10.1016/j.jhazmat.2020.122156.

Wang, J, Q Li, MM Li, TH Chen, YF Zhou, and ZB Yue (2014). "Competitive adsorption of heavy metal by extracellular polymeric substances (EPS) extracted from sulfate reducing bacteria". In: *Bioresource Technology* 163, pp. 374–376. ISSN: 18732976. DOI: 10.1016/j.biortech.2014.04.073. URL: http://dx.doi.org/10.1016/j.biortech.2014.04.073.

Whitman, WB (2010). *Bergey's Manual of Systematic Bacteriology*. ISBN: 9780387950426. DOI: 10.1002/jcc.540120406.

Worch, E (2012). *Adsorption technology in water treatment : fundamentals, processes, and modeling*. De Gruyter. ISBN: 9783110240238. DOI: 10.1515/9783110240238.11.

Wu, FC, RL Tseng, and RS Juang (2009). "Characteristics of Elovich equation used for the analysis of adsorption kinetics in dye-chitosan systems". In: *Chemical Engineering Journal* 150.2-3, pp. 366–373. ISSN: 13858947. DOI: 10.1016/j.cej.2009.01.014.

Xu, H, Y Chen, H Huang, Y Liu, and Z Yang (2013). "Removal of lead (II) and cadmium (II) from aqueous solutions using spent Agaricus bisporus". In: *Canadian Journal of Chemical Engineering* 91.3, pp. 421–431. ISSN: 00084034. DOI: 10.1002/cjce.21671.

Yang, J and B Volesky (1999). "Modeling uranium-proton ion exchange in biosorption". In: *Environmental Science and Technology* 33.22, pp. 4079–4085. ISSN: 0013936X. DOI: 10.1021/es990435q.

Yang, X, Y Wan, Y Zheng, F He, Z Yu, J Huang, H Wang, YS Ok, Y Jiang, and B Gao (2019). "Surface functional groups of carbon-based adsorbents and their roles in the removal of heavy metals from aqueous solutions: A critical review". In: *Chemical Engineering Journal* 366.January, pp. 608–621. ISSN: 13858947. DOI: 10.1016/j.cej.2019.02.119. URL: https://doi.org/10.1016/j.cej.2019.02.119.

Yang, ZX, SQ Liu, DW Zheng, and SD Feng (2006). "Effects of cadium, zinc and lead on soil enzyme activities". In: *Journal of Environmental Sciences (China)* 18.6, pp. 1135–1141. ISSN: 10010742. DOI: 10.1016/S1001-0742(06)60051-X.

Yee, N, DA Fowle, and FG Ferris (2004). "A Donnan potential model for metal sorption onto Bacillus subtilis". In: *Geochimica et Cosmochimica Acta* 68.18, pp. 3657–3664. ISSN: 00167037. DOI: 10.1016/j.gca.2004.03.018.

Zhang, P, YP Chen, MW Peng, JS Guo, Y Shen, P Yan, QH Zhou, J Jiang, and F Fang (2017). "Extracellular polymeric substances dependence of surface interactions of Bacillus subtilis with Cd2+ and Pb2+: An investigation combined with surface plasmon resonance and infrared spectra". In: *Colloids and Surfaces B: Biointerfaces* 154, pp. 357–364. ISSN: 18734367. DOI: 10.1016/j.colsurfb.2017.03.046. URL: http://dx.doi.org/10.1016/j.colsurfb.2017.03.046.

Zhao, G (2011). "Sorption of Heavy Metal Ions from Aqueous Solutions: A Review". In: *The Open Colloid Science Journal* 4.1, pp. 19–31. ISSN: 18765300. DOI: 10.2174/1876530001104010019.